CSIRO PUBLISHING

RESEARCH PAPER
https://doi.org/10.1071/WF21141

International Journal of WILDLAND FIRE

International Association of Wildland Fire

Comparison of fire-produced gases from wind tunnel and small field experimental burns

David R. Weise[A,*], Wei Min Hao[B], Stephen Baker[B], Marko Princevac[C], Amir-Hessam Aminfar[C], Javier Palarea-Albaladejo[D,E], Roger D. Ottmar[F], Andrew T. Hudak[G], Joseph Restaino[H] and Joseph J. O'Brien[I]

For full list of author affiliations and declarations see end of paper

***Correspondence to:**
David R. Weise
USDA Forest Service, Pacific Southwest Research Station, Riverside, CA 92507, USA
Email: david.weise@usda.gov

Received: 2 June 2021
Accepted: 15 February 2022
Published: 20 April 2022

Cite this:
Weise DR *et al.* (2022)
International Journal of Wildland Fire
31(4), 409–434. doi:10.1071/WF21141

ABSTRACT

Composition of pyrolysis gases for wildland fuels is often determined using ground samples heated in non-oxidising environments. Results are applied to wildland fires where fuels change spatially and temporally, resulting in variable fire behaviour with variable heating. Though historically used, applicability of traditional pyrolysis results to the wildland fire setting is unknown. Pyrolytic and flaming combustion gases measured in wind tunnel fires and prescribed burns were compared using compositional data techniques. CO_2 was dominant in both. Other dominant gases included CO, H_2 and CH_4. Relative amounts of CO, CO_2 and CH_4 were similar between fire phases (pyrolysis, flaming combustion); relatively more H_2 was observed in pyrolysis samples. All gas log-ratios with CO_2 in pyrolysis samples were larger than in flaming combustion samples. Presence of live plants significantly affected gas composition. A logistic regression model correctly classified 76% of the wind tunnel samples as pyrolysis or flaming combustion based on gas composition. The model predicted 60% of the field samples originated from pyrolysis. Fire location (wind tunnel, field) and fire phase affected gas composition. The compositional approach enabled analysis and modelling of gas compositions, producing results consistent with the basic characteristics of the data.

Keywords: compositional data analysis, flaming combustion, gas composition, GC/FID, logistic model, *Pinus palustris*, prescribed burning, pyrolysis.

Introduction

Wildland fire involves three main chemical processes – solid fuel pyrolysis, combustion of gaseous pyrolysis products and char combustion. In operational fire models in the United States, pyrolysis has not been explicitly included; however, fuel types containing live fuels that produce more volatiles than dead wood have higher heat content values to compensate for this omission (Rothermel and Philpot 1973; Hough and Albini 1978; van Wilgen 1984). As computational resources have increased, the treatment of pyrolysis and chemical reactions of combustion has been described mathematically and included in physics-based fire models (Grishin 1997; Zhou and Pereira 2000; Morvan and Dupuy 2004; Zhou *et al.* 2005; Mell *et al.* 2009; Clark *et al.* 2010; El Houssami *et al.* 2016; Morvan *et al.* 2018) including a recent coupling of the Gpyro and Fire Dynamics Simulator (FDS) models (Lautenberger and Fernandez-Pello 2009; Lautenberger 2014; Yashwanth *et al.* 2015, 2016).

Extensive literature exists about pyrolysis of biomass and its components (e.g. Broido and Kilzer 1963; Shafizadeh 1982; Antal 1985*a*, 1985*b*; Buessing and Goldfarb 2012; Kan *et al.* 2016; Wang *et al.* 2017; Pecha and Garcia-Perez 2020), particularly as related to potential energy sources. Studies of biomass from forests have tended to focus on wood and wood waste. For energy production, biomass is typically modified physically or chemically, so the applicability of the results to the wildland setting is uncertain with the possible exception of fuels produced by mechanical chipping and grinding to reduce fire risk (Kane *et al.* 2009; Knapp *et al.* 2011; Kreye and Kobziar 2015; Lyon *et al.* 2018).

The primary constituents of biomass (cellulose, hemicellulose and lignin) have been subject to intensive study individually (e.g. Collard and Blin 2014). Biomass pyrolysis can be classified based on heating rate and solid residence time (Kan *et al.* 2016; Pecha and Garcia-Perez 2020): slow (very low heating rate <1°C s^{-1}, 300–700°C, residence times of hours to days), fast (high heating rate >10–200°C s^{-1}, residence time of 0.5–10 s) and flash (heating rate 10^3–10^4°C s^{-1}, residence time <0.5 s).

Since the 1960s, thermogravimetric analysis (TGA) and differential scanning calorimetry (DSC) have been used to identify the components and kinetic properties for wildland fuels and their components (cellulose, hemicellulose and lignin) using both non-oxidising and oxidising atmospheres (e.g. Broido 1968; Shafizadeh *et al.* 1971; Duvvuri *et al.* 1975; Susott 1982; Statheropoulos *et al.* 1997; Dimitrakopoulos 2001; Liodakis *et al.* 2002; Font *et al.* 2009; Tihay and Gillard 2011; Costa *et al.* 2016; Amini *et al.* 2019*a*). TGA, DSC and other methods typically use fuel samples that have been ground to a fine powder and heated slowly, thus removing the effects of wildland fuel particle shape and high heating rate on the resulting product composition. These slow-heating methods have been applied to a wide range of wildland fuels (Susott 1982; Grishin 1997; Dimitrakopoulos 2001; Cancellieri *et al.* 2005; Font *et al.* 2009; Tihay and Gillard 2011; Korobeinichev *et al.* 2013; Wadhwani *et al.* 2017). In studies where fast and flash pyrolysis have been used to characterise pyrolysis products, fuel samples, forest residues and organic soils have also been typically ground or modified in some manner (Bracewell 1971; Jarvis 1995; Statheropoulos *et al.* 1997). Less common are pyrolysis experiments using intact wildland fuels that included the above-ground components of trees, shrubs and grasses as well as peats and organic soils (Roy *et al.* 1983; Chetehouna *et al.* 2009, 2012, 2013; Bartoli *et al.* 2011; Hadden *et al.* 2013; Safdari *et al.* 2018, 2019, 2020). Reported air heating rates near foliar fuels in wildland fire range from 30 to 5000°C s^{-1} (Martin and Davis 1961; Rothermel 1972; Butler *et al.* 2004, 2016; Tachajapong *et al.* 2008). While a fuel particle will not necessarily heat at the same rate as the adjacent air owing to its thermal properties (Huggett 1984) and the nature of the heat transfer method (Cohen 2015; Finney *et al.* 2015), the rate of temperature rise in wildland fuel particles is more akin to fast pyrolysis rates. Higher heating rates and high temperatures are also typical of pyrolysis in wood-based structures (Moghtaderi 2006).

Prior pyrolysis work has argued the need to conduct experimental work under well-controlled conditions owing to the complexity of thermal behaviour chemically and physically as opposed to conducting this work during actual fires under field conditions with limited control of conditions (Dimitrakopoulos 2001). However, we find no quantitative comparison of results from well-controlled experiments with results from actual fires to support this approach. To test this assumption, measurements of pyrolysis are needed for actual fires under field conditions with limited control. A project to compare results from well-controlled bench-scale experiments with less-controlled larger-scale (wind tunnel, field) experiments is nearing completion (Weise *et al.* 2018). Bench-scale results from slow (TGA-like) and fast (flat-flame burner) heating rates are available (Safdari *et al.* 2018, 2019, 2020; Amini *et al.* 2019*a*, 2019*b*, 2021; Weise *et al.* 2021). Results of pyrolysis measurements of the larger-scale fires using Fourier-transform infrared (FTIR) spectroscopy are available (Scharko *et al.* 2019*a*, 2019*b*; Phillips *et al.* 2020; Banach *et al.* 2021). The present paper compares gases collected in canisters quantified by gas-chromatography/flame ionisation detector (GC/FID) analysis between the two larger-scale experiments.

Methods

Gas samples collected from experimental fires in simplified fuel beds occurred in a low-speed wind tunnel at the Forest Service research laboratory in Riverside, California, USA and small field-scale prescribed burns (0.1 ha) at Fort Jackson in South Carolina, USA and the Tall Timbers Research Station Pebble Hill Plantation in Georgia, USA comprise the gas data presented here. The Forest Service wind tunnel includes environmental control and a 2 m test section (Bartolome *et al.* 2019) where fuel beds can be burned.

Fire and fuel description

Wind tunnel

Eighty-eight fuel beds 2.4 m long and approximately 0.8 m wide composed of longleaf pine (*Pinus palustris* Mill.) needles and various combinations of fetterbush (*Lyonia lucida* (Lam.) K. Koch), sparkleberry (*Vaccinium arboreum* L.), blueberry (*V. darrowii* Camp) and inkberry (*Ilex glabra* (L.) A. Gray) plants (Appendix Table A1) were burned under 0 and 1 m s^{-1} wind conditions between November 2017 and November 2018. Fuel beds were constructed by uniformly distributing 1000 g (wet weight) of needles over the entire fuel bed in sections based on a well-established procedure (Anderson and Rothermel 1965; Schuette 1965; Rothermel and Anderson 1966) and then placing the plants in predetermined locations (Fig. 1). Composition and characteristics of the fuel bed components are available (Safdari *et al.* 2018; Matt *et al.* 2020). Fuel moisture content (ASTM International 2016) of foliage and longleaf pine needles was determined using a Computrac® MAX 2000XL[1] and a convection oven, respectively (Haase *et al.* 2016). Immediately prior to

[1]The use of trade or firm names in this publication is for reader information and does not imply endorsement by the US Department of Agriculture of any product or service.

ignition, ambient temperature and relative humidity were measured using a Kestrel 3000 pocket weather meter. Air temperature, relative humidity and dewpoint in the wind tunnel at the upwind end of the test section were measured every 5 min by a Vertiv™ Geist™ Watchdog 15 environmental monitor. Fuel beds were ignited with a line fire that spread the length of the fuel bed. Each fire achieved quasi-steady state rate of spread within 0.3 m of the upwind edge of the fuel bed. Rate of spread was determined by dividing the fuel bed length by the time required for the fire to spread the entire length. Vertical total and radiant heat fluxes into the fuel bed were measured using two identical Medtherm 64 series Schmidt–Boelter type sensors located upwind and downwind of a plant placed on an electronic scale to measure mass loss (Fig. 1*b*). Horizontal convective flux to the plant foliage was estimated (Aminfar *et al.* 2020) as direct measurement was not possible. Fuel temperatures during the preheating process and prior to ignition were measured using FLIR Systems T640 (wind tunnel) and A655 (field) long-wave thermal infrared imagers. For the wind tunnel (T640), a point sample of the uncorrected radiant temperature of a leaf near the FTIR gas sampling probe (Banach *et al.* 2021) was extracted from the same pixel in each image. Maximum heating rate was estimated as the maximum positive slope of the temperature–time plot; maximum fuel temperature was determined from these data. An ocular estimate of flame height was made using wind tunnel height (1 m) as a reference.

Field fires

Five 0.1 ha experimental plots located at Fort Jackson near Columbia, SC, in longleaf pine–slash pine forests (*P. elliottii* Engelm.) were burned in May 2018. Two plots were burned on the Pebble Hill Plantation of the Tall Timbers Research Station near Tallahassee, FL, in April 2018. Fall-line Xeric Longleaf Woodland and Southern Subxeric Longleaf Woodland describe the coarse differences between vegetation at Fort Jackson and Pebble Hill Plantation, respectively (Peet and Allard 1993; Ostertag and Robertson 2007). The dominant understorey shrub in the Fort Jackson plots was sparkleberry. Eight paired clip plots 1 × 1 m in area were systematically arranged in four of the 0.1 ha burn units to measure shrubs, grass, fine downed woody debris (<7.62 cm diameter), litter and duff. Soil organic matter at Fort Jackson had a large component of incorporated sand so duff mass loading was estimated using a depth–mass relationship developed from the nearby Sumter National Forest for loblolly pine (*P. taeda* L.) stands (Ottmar and Andreu 2007). Fuel data were collected less than 1 week prior to each burn and within 2 days after each burn to minimise changes in fuels. Fuel moisture sampling occurred immediately prior to and during ignition. The fuel moisture samples were stored in air-tight sample containers and processed in a convection oven (ASTM International 2016). Geometric means and standard deviations were calculated for loading and fuel moisture data for each 0.1 ha burn unit.

Fire behaviour was variable in the field burns owing to variably spaced strip head fires to keep fire intensity low enough for personnel to approach the flames safely (Waldrop and Goodrick 2012). Based on occasional ocular estimates, flame lengths were quite variable, ranging from 0.3 to 2 m and were affected by the distribution of sparkleberry, which increased flame length within each burn unit. With little to no wind, visually estimated rate of spread was 0.01–0.02 m s^{-1}, similar to other field measurements (Johansen 1987; Robertson and Ostertag 2007) and consistent with the wind tunnel experiments (Appendix Table A1). Further description of the plots and experimental burns is available (Scharko *et al.* 2019*a*; Hudak *et al.* 2020).

Pyrolysis gas sampling

Separate, clean, evacuated SUMMA® polished 0.85 L canisters were used to collect and store sampled gases for each wind tunnel and field fire. Final pressure in each canister was approximately 25 psia (pounds per square inch absolute, 172 kPa). These canisters are viable collection and storage media up to 32 weeks for the observed gases (Evans *et al.* 1998) and are used routinely for fire gas sampling (e.g. Austin *et al.* 2001; Wang *et al.* 2014; Strand *et al.* 2016).

Wind tunnel fires

Sampling pyrolysis gases in an open-air environment is a challenge as pyrolysis is a transient process. The present study collected composite samples, eliminating the temporal component. The sampling approach yielded 'fire-averaged' samples, which is a standard approach for smoke sampling (Ward and Radke 1993; Wooster 2003; Simpson *et al.* 2011; Garofalo *et al.* 2019). An array of eight stainless-steel tubes connected to a pump/manifold collection system with a 100 mL s^{-1} sample flow rate arose from the base of the wind tunnel through the fuel bed (Fig. 1). A 5 µm stainless steel filter removed particles upstream of the pump. Separate switches controlled each sample tube. Given the short distance between the sample tube inlet and the canister (<3 m) and the high flow rate, the sample line was not heated. At sample tube 'F', flaming emissions (smoke) were collected in a canister for 30 s before the flame reached the sample tube. While pyrolysis gases may have been entrained into the plume and included in the flaming sample, the preponderance of gases resulted from flaming combustion because the plume extended downstream of the visible flame (Aminfar *et al.* 2020). The flaming canister was then replaced by a new canister. A verbal command to initiate and end sampling at the 'P' sample tubes based on fire progression resulted in a short sampling interval at each tube prior to flame front arrival. The plume was well above the tube inlet so minimal amounts of flaming combustion gases were collected. Each pyrolysis canister was filled with multiple small aliquots from the seven 'P' sample

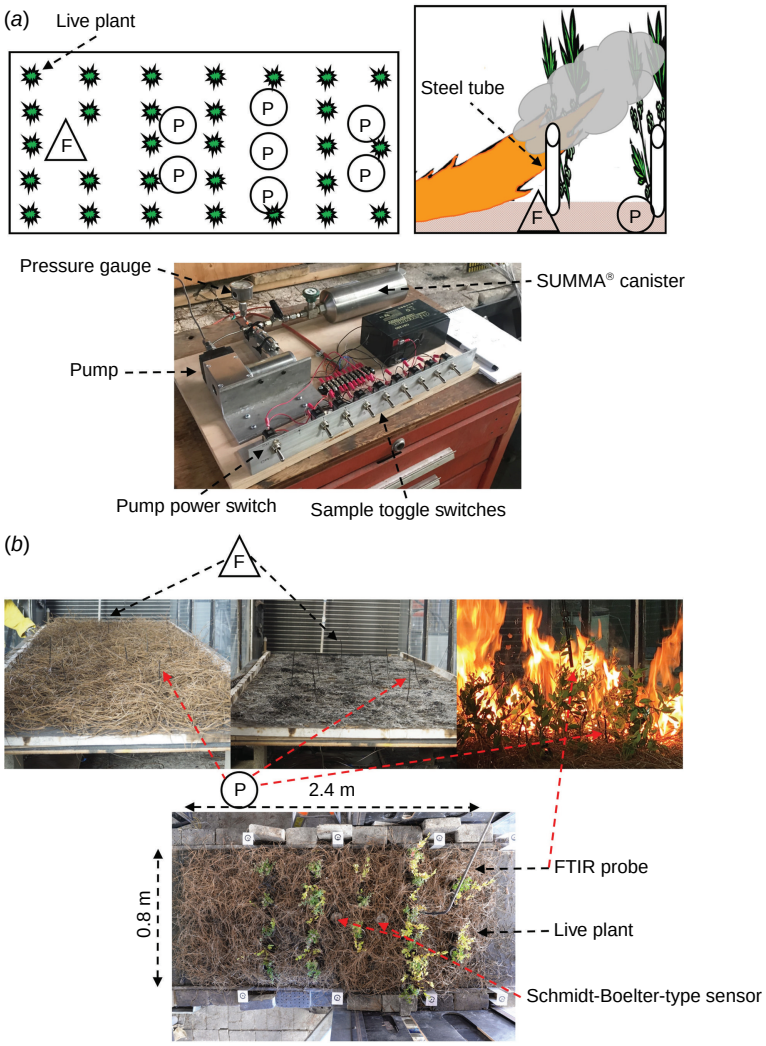

Fig. 1. (*a*) Wind tunnel canister gas-sampling system used to sample pyrolysis and flaming combustion gases from long-leaf pine needle fuel beds through stainless steel tubes. 'F' and 'P' denote the approximate locations of the flaming combustion and pyrolysis sample tubes, respectively. Live plant location is also approximate. Not drawn to scale. (*b*) Pine needle fuel bed before (left), and after (middle) burning with sample tubes identified. Sample tubes in burning fuel bed (right). Pyrolysis sample collected before flame arrived. Overhead view of fuel bed shows additional sensors used in experiments.

tubes. Contamination of 'P' samples by residual smouldering gases was non-existent. Between each fire, ambient air was pumped through the sampling system for 30 min to purge any residual gases. Sampling gases from replicated experiments with controlled fuel bed composition, quasi-steady state repeatable heating conditions (flame) and sequentially collected gas samples from several points along the length of the fuel bed as the flame advanced limited the variability of the gas composition from the seven pyrolysis samples. The canister content is assumed to be representative of the sample points. The gases sampled were light hydrocarbons up to C_7 and a few aromatics that were stable in the sampling line and canisters. Condensable compounds ('tars') could condense in the canister but did not affect the gas analysis; these compounds were removed from the canisters by the cleaning process performed at the Forest Service Missoula Fire Sciences Lab between the three sets of experimental fires. For 65 of the 88 wind tunnel fires, a paired sample of a flaming canister and a pyrolysis canister was collected. Of the remaining 23 fires, there were 21 and 2 canisters containing only pyrolysis or flaming gases, respectively. These canisters were processed offline as described below.

Field fires

To safely sample gases during the prescribed burns, we used a gas sampling probe built from 2.5 m of 6-mm stainless-steel tubing connected to the sampling package with flexible stainless tubing. A swing Piston KNF Neuberger Pump, 12-V gel cell rechargeable battery and stainless-steel tubing coupled to a pressure relief valve and gauge comprised the sampling package. The flow rate to fill the SUMMA® canisters was 250 mL s^{-1}. A remotely triggered sampling system such as FASS (Susott *et al.* 1991; Ward *et al.* 1992) was not practical for this study as expert judgement was needed to locate the sample probe to increase the probability of collecting pyrolysis gases. The sampling strategy was to identify plants with sufficient foliage along the edge of the burn unit where they could be safely sampled. At the base of the advancing flame, the probe collected short-interval sample aliquots when it was likely that pyrolysis was occurring.

Owing to this uncertainty, the field samples were not initially labelled as flaming or pyrolysis samples; subsequent statistical analysis classified these samples.

Gas chromatography

All canisters were analysed using Environmental Protection Agency (EPA) method TO-14A (EPA 1999) for CO_2, CO, CH_4, and C_2 to C_7 hydrocarbon gases with an Agilent model 7890 gas chromatograph configured with two columns running simultaneously. A 3.175 mm diameter, 2 m Carbosphere packed column with a nickel catalyst methaniser was used for analysis of CO_2 and CO using flame ionisation detectors (FIDs). The second column, a 0.53 mm diameter × 50 m length Agilent Al/S column, separated hydrocarbons and methane. Both columns went to FID detectors and were run simultaneously. Chromatogram data were collected and processed by Agilent OpenLab software. A multipoint set of three standards bracketing the sample concentrations were analysed with each set of samples to construct a standard curve for each compound. Based on the integrated peak areas, sample concentrations were calculated from the standard curves. National Institute of Standards and Technology (NIST) standard reference material (SRM) gas standards for CO, CO_2, CH_4 and propane were run each day to validate the standard curve (Montgomery and Crivellone 2021). Duplicate GC runs of canisters were performed for each sixth sample. For measurement of H_2 concentration, a Trace Analytical RGA3 reduction gas analyser was used (Jordan and Steinberg 2011). This chromatographic instrument with a molecular sieve column and UV mercuric oxide detector provided highly sensitive precise measurement of trace-level H_2; the range of detection is 0–10 ppm H_2 and most samples were diluted with ultra high purity (UHP) nitrogen to be in this range. A 10 ppm H_2 standard (Scott Specialty Gases) was diluted to a 1–3 ppm calibration standard, which exceeds average ground level concentration of 0.6 ppm (Glueckauf and Kitt 1957). Chromatograms of H_2 from this instrument were collected and integrated with Agilent OpenLab software interfaced to the instrument. The H_2 measurement was highly precise with an estimated overall error of 5%. On a subset of canisters with significant detectable pyrolysis gases, GC–mass spectrometry (GC/MS) analysis was performed using an Agilent 6890 GC with an HP-5 0.320 mm × 30 m column, He carrier gas and Agilent 4590N MS detector. The excess mixing ratios for each gas induced by a fire (Ward and Radke 1993; Urbanski *et al.* 2008) resulted from background air samples and the analysed canisters. A total of 195 canisters was analysed for gas composition in the wind tunnel (88 pyrolysis, 65 flaming) and field burns (42).

Statistical analysis

Smoke and pyrolysis data are compositional data (Weise *et al.* 2020*a*, 2020*b*, 2021) and were analysed as such. All statistical analyses were performed using R 3.6.3 (R Core Team 2020. 'R: A Language and Environment for Statistical Computing.' (R Foundation for Statistical Computing: Vienna, Austria), https://www.R-project.org/).

The measured gases comprised 29 gases with observations in the data set containing values below detection limit (BDL) for most gases. Hexane, furan, 1-hexene, heptane, benzene, toluene and furfural displayed >98% BDL values and were discarded from subsequent analysis. The remaining 22 gases were preprocessed using the *multLN* function to impute random values below the minimum observed concentrations (Palarea-Albaladejo and Martín-Fernández 2013, 2015) as rounded zeroes are problematic in log-ratios. The compositional centre (mean) and total (metric) variance were estimated (Aitchison 1986). Gas composition data were transformed using *ilr* transformations (Egozcue *et al.* 2003). Sequential binary partitioning defined meaningful contrasts (balances) between subsets of the gases. A balance is simply the planned comparison between two groups of gases (in this case) that are of interest to the experimenter (Egozcue and Pawlowsky-Glahn 2005). It is analogous to comparing the means associated with the levels of a treatment as is typically done in a designed experiment (Mason *et al.* 1989).

Analysis of the *ilr*-transformed coordinates consisted of the following steps:

1. Mixed effects modelling to test if the fire effect (repeated measurement of gas composition in two canisters as a random effect) significantly affected the gas composition (multivariate response) was performed.
2. The fire effect was not statistically significant so the significance of fuel bed (fixed effect) and covariates for wind tunnel conditions on gas composition was tested.
3. Logistic regression related the probability a wind tunnel canister was pyrolysis or flaming combustion (fire phase) to the measured gas composition.
4. Model fit from Step 3 predicted fire phase of the field canisters.
5. Effects of the fixed effects for fire phase and location (wind tunnel or field) on gas composition were tested using all canisters.

For Step 1, a multivariate linear mixed effects model (McCullagh and Nelder 1998; Pinheiro and Bates 2000) was fitted using the *lmer* function (Bates *et al.* 2015). The response variable was the gas composition (multivariate); statistical significance of the random fire effect was tested using the *ranova* function (Kuznetsova *et al.* 2017) and the *anova* function was used to test statistical significance of fixed effects and covariates.

For Step 2, a multivariate linear model with covariates for fuel moisture content, relative humidity and air temperature and a fuel bed fixed effect was fitted. Understanding the fuel bed effect on individual gases was accomplished by transforming the fitted values back into compositions by

Table 1. Schematic illustrating the construction of balances of gases determined by sequential binary partition. '+' and '−' denote gases in the numerator and denominator of a balance.

Balance	H_2	CO	CO_2	CH_4	Alkanes	Alkenes	Alkynes
Zhou vs NMOC[A]	+	+	+	+	−	−	−
H_2 vs CO_2, CO, CH_4[B]	+	−	−	−			
CO_2 vs CO, CH_4		−	+	−			
CO vs CH_4		+		−			
Alkanes vs other NMOC[C]					+	−	−
Alkenes vs alkynes						+	−

[A]Zhou refers to a reduced combustion mechanism containing H_2, CO, CO_2 and CH_4 (Zhou and Mahalingam 2001). NMOC is non-methane organic compounds.
[B]H_2 compared with the gases in Westbrook–Dryer combustion mechanism (Westbrook and Dryer 1981).
[C]Alkanes – C_2H_6, C_3H_8, C_4H_{10}, C_5H_{12}; alkenes – C_2H_4, C_3H_6, C_4H_8, C_5H_{10}; alkynes – C_2H_2, C_3H_4, C_4H_6.

inverse *ilr* transformation (Egozcue *et al.* 2003) and plotting the average deviation (Eqn 1) for each gas i in barplots,

$$\left(\text{average deviation}_{\log\ \text{scale}}\right)_i = \log\left(\frac{\left(\hat{g}_{\text{effect}_k}\right)_i}{\hat{g}_i}\right), \quad i = 1, \ldots, D;\ k = 1, \ldots, m \quad (1)$$

where m is the number of levels of effect k and $\hat{g}$, $\hat{g}_{\text{effect}_k}$ denote the overall geometric mean of and the geometric mean for each effect level k for each gas i, respectively (Montero-Serrano *et al.* 2010; Butler *et al.* 2020). Analogous analysis of the fuel bed effect on defined groups of gases (balances) (Table 1) was done. As we were examining two reduced reaction mechanisms (Dryer and Glassman 1973; Westbrook and Dryer 1981; Zhou and Mahalingam 2001; Leroy *et al.* 2008; Andersen *et al.* 2009; Tihay *et al.* 2009) for pyrolysis and combustion in a related modelling study (Borujerdi 2021), we chose to test the effects of fuel bed on the gases making up these reduced mechanisms. The effect of fuel bed on the relative amounts in different non-methane organic compound (NMOC) gas categories (alkanes, alkenes, alkynes) was also of interest as at least one other study has reported differences between fuel beds (Urbanski *et al.* 2008). It is important to note that average deviation and average difference (for balances) plots suggest trends and are not statistical tests. Pairwise *t*-test comparisons of the effects for the balances were performed using the *glht* function (Hothorn *et al.* 2008; Bretz *et al.* 2011) with adjusted *P*-values to control the false discovery rate (Benjamini and Hochberg 1995).

For Step 3, a logistic regression model relating gas composition in *ilr*-coordinates to the known probability (86/153 or 0.562) that a canister was a pyrolysis sample was developed using the *glm* function with a logit link function and binomial error distribution. In Step 4, the fitted logistic model predicted the fire phase of each field sample using the measured gas composition. In Step 5, a multivariate linear model with fixed effects for fire location (wind tunnel, field) and fire phase (pyrolysis, flaming combustion) was fitted to test the statistical significance of these variables. Pairwise comparisons were performed as above. Effects were plotted as average deviations for the individual gases and as average differences for the balances.

Results and discussion

In total, 88 fires were burned in the wind tunnel. Characteristics of the 88 fires are summarised in Appendix Table A1. The wet fuel loading of the longleaf pine needles was typically 500 g m^{-2}, mean (min, max) fuel moisture content of the needles was 9.8% (6, 15.6%) and of the live foliage was 112.5% (73.2, 173.6%). In the wind tunnel, environmental conditions simulated growing season (dead fuel moisture 9.6%, air temperature 297 K, relative humidity 35%) and dormant season (dead fuel moisture 10.6%, air temperature 280.6 K, relative humidity 63%) conditions. Fuel loading as well as ambient temperature and relative humidity in the wind tunnel varied between experiments (Appendix Table A1). Longleaf pine needle dry loading ranged from 431 to 472 g m^{-2} after correcting for moisture content. The nursery plants were seedlings and quite small (Appendix Table A2). Dry mass of the live plants was not measured. Assuming the dry mass of the stem and foliage of a single plant ranged from 5 to 20 g results in an estimated live plant dry mass ranging from 125 to 1500 g and a loading of 83 to 1000 g m^{-2}. Low-density fuel beds contained up to 50 plants and high-density fuel beds contained 74 plants. Although the moisture content of the live plants was appreciably higher than for the pine needles, the pine needles were the primary fuel for fire spread as is typical in southern pine stands and other coniferous forests throughout the world. Harmonic mean spread rate of all fires was 0.008 (0.004–0.027) m s^{-1}.

In the wind tunnel, ocularly estimated flame heights for the no-wind fires ranged from 0.3 to 0.6 m with an estimated flame depth of 0.3 m based on a residence time of 28 s derived from an average longleaf pine needle diameter of 0.0015 m (Fons *et al.* 1963; Snyder and Hamaker 1978;

Alexander and Cruz 2011). Flame heights for the wind-aided fires were similar and the flame lengths were longer. An overhead view of a fuel bed containing inkberry and the flame for a no-wind fire can be found elsewhere (Banach *et al.* 2021). Vertical total and radiant heat fluxes from the flame into the fuel bed ranged up to 25 and 14 kW m^{-2}, respectively (Aminfar 2019). Estimated horizontal convective fluxes from the plume to the leaves ranged up to 0.8 kW m^{-2} (Aminfar *et al.* 2020). The mean spread rate, longleaf pine heat of combustion (19 000 kJ kg^{-1}) (Dietenberger *et al.* 2020), dry fuel loading (0.45 kg m^{-2}) and flame depth (0.3 m) yielded a fireline intensity of 68 kW m^{-1} and combustion rate of 228 kW m^{-2} (Byram 1959; Alexander and Cruz 2011). These flame heights and fireline intensities fall at the lower end of the range reported for low-intensity prescribed burns in southern fuel beds (Nelson 1980; Wade 1993; Nelson *et al.* 2012) and resulted in fuel heating rates consistent with fast pyrolysis (Appendix Table A1).

Wind tunnel and field fuel beds differed in complexity, containing 2 and 10 components, respectively (Appendix Table A3). Fuel loading data are also compositional, so results are reported accordingly. Duff, the dominant component of preburn fuel loading at Fort Jackson, comprised a mean proportion of 0.594 of the fuel loading. The shrub component was significant both visually and from a fire behaviour perspective (Zylstra *et al.* 2016), but it was generally a minor part of the fuel bed composition by weight, even if not by volume (Hudak *et al.* 2020). The shrub component proportion was 0.014. After the burns, the proportions for duff and shrub components were 0.957 and 0.003, respectively. The preburn log-ratio of shrub to litter loading at Fort Jackson was −3.2 while the same log-ratio in the wind tunnel ranged from −1.8 to −0.7. Based on this one log-ratio, wind tunnel fuel beds contained more shrub material relative to longleaf litter than the natural fuel beds.

Geometric mean concentrations for wind tunnel and field gas samples ranged over seven and eight orders of magnitude, respectively (Appendix Table A4). The original concentrations were summarised as geometric mean ⋇ geometric standard deviation, denoting the multiplicative scale of the variables (Butler *et al.* 2020). CO_2 was the dominant gas observed in the canister samples followed by CO, H_2 and CH_4 (Appendix Table A4). Whereas the relative concentrations of CO, CO_2 and CH_4 in the wind tunnel were similar between the pyrolysis and flaming combustion samples, the relative concentration of H_2 doubled in the pyrolysis canisters (Fig. 2). Fig. 2 suggests a meaningful relationship between the geometric mean hydrocarbon concentrations and molecular weight. This is similar to a regression developed in Yokelson *et al.* (2013, eqn 1) between observed molecular mass and number of C atoms in identified compounds in biomass smoke. Linear regression can be used to investigate the association of compositional data with one or more predictor variables (van den Boogaart and Tolosana-Delgado 2013; Weise *et al.* 2020*b*) after applying an *ilr* transformation; however, formally relating molecular weight with the mean relative concentrations in this figure is problematic because there were 18 *ilr* coordinates (log-ratios each involving several concentrations) and 19 molecular weights (referring to each one of the individual gases). Ignoring the compositional aspect at this point, we fitted the $\log_{10}$ of the mean concentrations to molecular weight treating the concentrations as if they were independent data points; the adjusted R^2 was 0.30 and 0.36 for the pyrolysis and flaming data, respectively. Relative concentration of many of the higher molecular weight trace gases was greater in the pyrolysis samples, likely due to the decreased relative amount of CO_2. The relative amounts of isobutane and isopentane varied greatly, accounting for 43.2% of the total variance in the data (Appendix Table A4). In the so-called variation arrays (Appendix Table A5) for pyrolysis and flaming combustion samples, a mean log-ratio less than 0 indicated that the amount of the gas in the numerator was relatively smaller than in the denominator. Based on this criterion, less CH_4 (−5.0) was present than H_2 (−4.1) relative to CO_2 in the pyrolysis samples. The log-ratios of CH_4 to H_2 in the pyrolysis (−0.9) and flaming combustion (−0.4) samples also show that less CH_4 relative to H_2 was present in the flaming wind tunnel samples, suggesting that relatively more of the H_2 was oxidised. The relatively greater concentration of H_2 is important to note as most pyrolysis modelling considers CH_4 to be more abundant (e.g. Di Blasi 2008) based on mass fraction, which is also a relative measure but is viewed as an absolute measure.

Paired sample effect

The random effect for the paired measurements in the wind tunnel was not statistically significant ($\chi^2 = 0$, P-value = 1); however, analysis of variance (ANOVA) showed a statistically significant difference in the *ilr* coordinates between pyrolysis and flaming phase samples (F-value$_{1,128}$ = 15.88, P-value = 0.0001), which was suggested by the relative concentrations (Fig. 2). All mean log-ratios of the gases with CO_2 were larger for the pyrolysis samples compared with the flaming samples, indicating that relatively more of each individual gas was present in the pyrolysis samples (Appendix Table A5).

Fuel bed effect

As gas composition differed between pyrolysis and flaming combustion, analysis of the effect of fuel bed on pyrolysis composition was restricted to the 86 wind tunnel pyrolysis samples. Multivariate analysis of variance, a global approach comparing equality of the means for each gas for each fuel bed type simultaneously, indicated that the fuel bed effect was statistically significant (Appendix Table A6). This means that the mean values of the *ilr* coordinates associated with the composition were not equal between fuel types in some

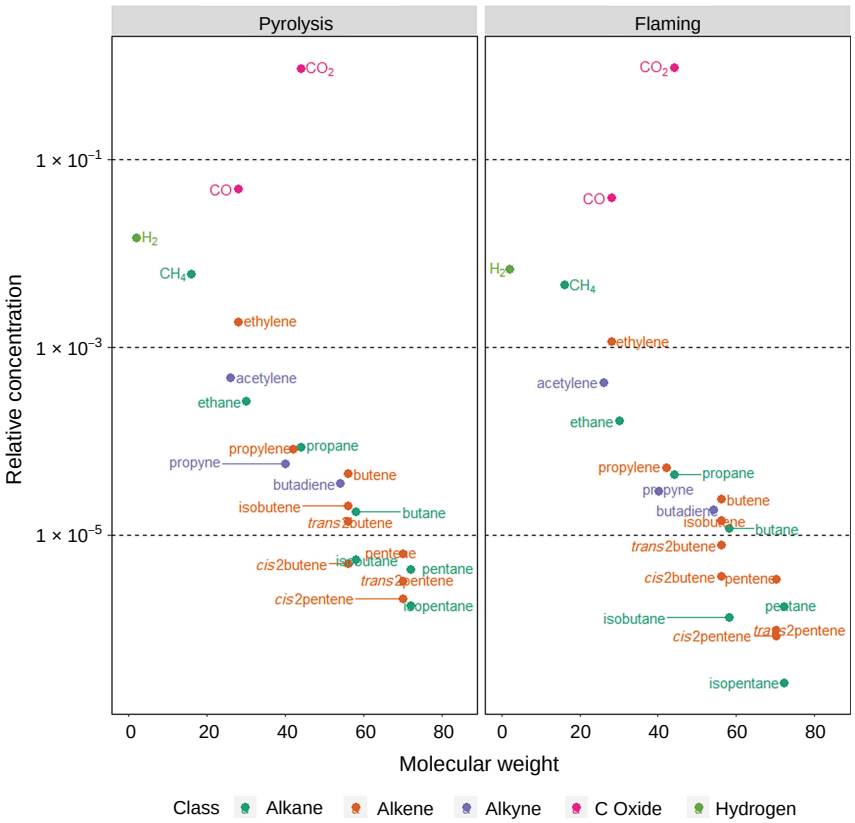

Fig. 2. Observed mean composition of samples of pyrolysis and flaming combustion gases in wind tunnel fires by chemical class after closure.

manner based on an *F*-test. None of the environmental variables affected the composition of pyrolysis gases. Based on the ANOVA parameterisation, the intercept term (not shown) represented the longleaf needle fuel bed with no live plants. The fuel bed effect captured the change in pyrolysis composition (all gases collectively) caused by the addition of live plants to the longleaf pine needles. The average deviation plot (Fig. 3) illustrated the relative differences in the estimated effect of each fuel bed type on the individual gases. For several gases, the mean of sparkleberry relative to the overall mean often had the largest (or smallest) average deviation compared with the other fuel beds.

Based on the pairwise comparisons between fuel bed types, fuel bed significantly affected the relative amount of alkanes compared with the other NMOCs (Table 2). Sparkleberry fuel beds produced relatively more alkanes (C_2H_6, C_3H_8, C_4H_{10}, C_5H_{12}) than other NMOCs (C_2H_2, C_2H_4, C_3H_4, C_3H_6, C_4H_6, C_4H_8 and C_5H_{10}). Overall, these results suggest that fuel bed did not significantly affect the composition of the dominant pyrolysis gases in the wind tunnel even though live plant mass may have ranged as high as 30% of the total fuel bed mass. The lack of an effect of fuel bed on the Zhou and Westbrook balances suggests that these mechanisms might be used in modelling for a variety of fuel bed types containing longleaf pine needles. The trace gas composition was affected by fuel bed type.

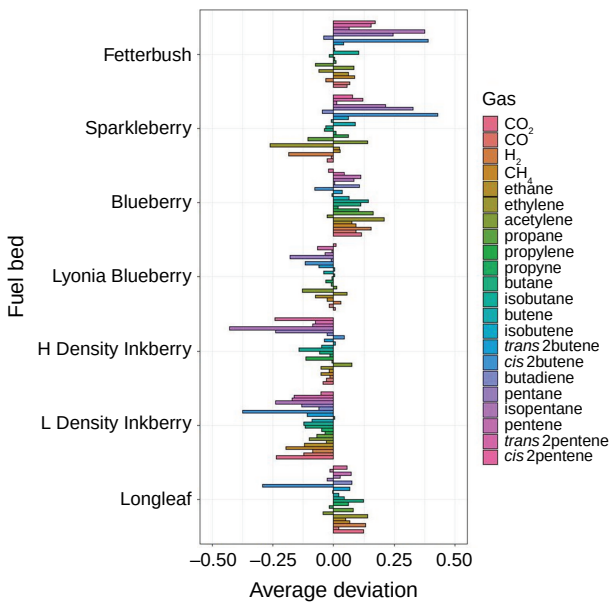

Fig. 3. Average deviation (log-ratio scale) by fuel bed type for pyrolysis gases sampled from experimental fires in a low-speed wind tunnel. H Density and L Density inkberry fuel beds had 74 and 50 plants per fuel bed, respectively.

Pyrolysis versus flaming combustion classification

Based on the number of canisters collected, the probability that a wind tunnel sample was pyrolysis was 86/153

Table 2. Pairwise comparisons of fuel bed effect on selected balance values for pyrolysis gases measured in a wind tunnel. Fuel beds that did not differ are indicated by the same letter with the letter values ordered from smallest to largest. *P*-values adjusted to control for false discovery rate at 0.05 (Benjamini and Hochberg 1995).

Balance[A]	Longleaf	Low Inkberry	High Inkberry	Fetterbush Blueberry	Blueberry	Sparkleberry	Fetterbush
Zhou vs NMOC	13.6a	14.9a	14.0a	13.6a	12.6a	13.6a	12.9a
H_2 vs CO_2, CO, CH_4	3.2a	4.2a	3.6a	4.0a	3.1a	2.9a	3.4a
CO_2 vs CO, CH_4	0.0a	−0.4a	−0.1a	−0.4a	−0.2a	0.0a	0.0a
CO vs CH_4	1.3a	1.2a	1.4a	1.4a	1.8a	2.1a	1.5a
Alkanes vs other NMOC	−2.3ab	−3.1a	−1.4ab	−3.3ab	−2.9ab	3.4c	0.4bc
Alkenes vs Alkynes	−2.8a	−2.3ab	−2.7a	−2.8ab	−3.2a	−1.1b	−1.9ab

[A]See Table 1.

or 0.562. All wind tunnel fires were used to fit a logistic regression model to predict the probability a sample resulted from pyrolysis using the composition of 22 gases in the sample as the predictor. The model was statistically significant ($\chi^2 = 41.77$, d.f. = 21, P-value = 0.004). The fitted model correctly classified 49 of 67 and 68 of 86 flaming and pyrolysis wind tunnel samples, respectively, for an overall correct classification rate of 117/153 or 76%. The model then classified 17 (2 Tall Timbers, 15 Fort Jackson) and 25 (6 Tall Timbers, 19 Fort Jackson) of the 42 field samples as flaming and pyrolysis samples, respectively.

Combining the known fire phase wind tunnel canisters and the predicted fire phase field canisters produced a data set of 195 canisters. Fire phase and location (wind tunnel, Tall Timbers, Fort Jackson) affected the composition of the canister gas samples (Appendix Table A7). Generally, the field effect at Fort Jackson was smaller than the wind tunnel effect as indicated by average deviations less than zero (Fig. 4). Recall that CO_2 comprised more than 92% of the samples (Appendix Table A4). Although it dominated the composition, there was relatively little difference between the locations. For the other dominant gases (CO, CH_4, H_2), the average deviation differed appreciably between Fort Jackson and the wind tunnel. Relatively more of these gases were present in the wind tunnel samples. This trend was noted for many of the 22 measured gases. A clear pattern was noted in the effect of fire phase on gas composition (Fig. 5). For all gases except CO_2, the average deviation for pyrolysis samples was greater than zero, indicating relatively more of the gases were present in the pyrolysis samples. For CO_2, the flaming samples had an average deviation greater than zero, indicating that relatively more CO_2 was observed in these samples. The lower concentration of many of the trace gases in the field samples for both pyrolysis and flaming combustion can be easily seen in Fig. 6.

The ANOVA results contained in Appendix Table A7 apply to both the default *ilr* transformation and the balances between subsets of gases (normalised ratios between their geometric means). While the bar plots illustrate the effects relative to the overall means, the multiple comparison tests for the balances indicated that more H_2 relative to the other dominant gases, less CO_2 relative to CO and CH_4 and less alkanes relative to other NMOCs were measured at Fort Jackson compared with the wind tunnel (Table 3). The relative amounts of dominant gases vs NMOC, CO vs CH_4 and alkenes vs alkynes did not differ between the wind tunnel and field canisters.

In the wind tunnel experiment, the fuel bed mass was dominated by longleaf pine needles. The percentage of mass of the fuel bed that consisted of live plants is unknown, but it was probably less than 30% given the fairly small size of the plants. In several burns, we added extra plants in the hope of producing a stronger signal due to the presence of the plants. This was successful because the composition of the gases in the wind tunnel differed between fuel beds. The relative amounts of each gas changed and some groupings by fuel bed were noted. Differences were observed in the relative amounts of the NMOCs; relative amounts of CO, CO_2, CH_4 and H_2 did not differ between fuel beds. Earlier work on the chemistry of wildland fuels noted differences in the chemical composition of the extractives, and our more recent bench-scale work (Matt *et al.* 2020; Weise *et al.* 2021) has also confirmed that the composition of both the fuel and the resulting gases released by pyrolysis does differ in the plants we examined. These results suggest that the anecdotal (and accepted) differences in fire behaviour characteristics of the different shrubs may be due in part to the NMOC component (as leaf shape was similar between species).

Comparison of the wind tunnel results with similar studies proved challenging for two reasons. As mentioned previously, there is a limited number of studies examining pyrolysis that measured similar compositions of gases. For example, Chen *et al.* (2010) studied both dead and living fuel samples and found that fuel moisture had an effect on smoke emissions. The only common gas reported in their study is CO and the study sampled gases from the smoke plume. Another study examined the impact of moisture content and plant species on boiler emissions of CO, NO

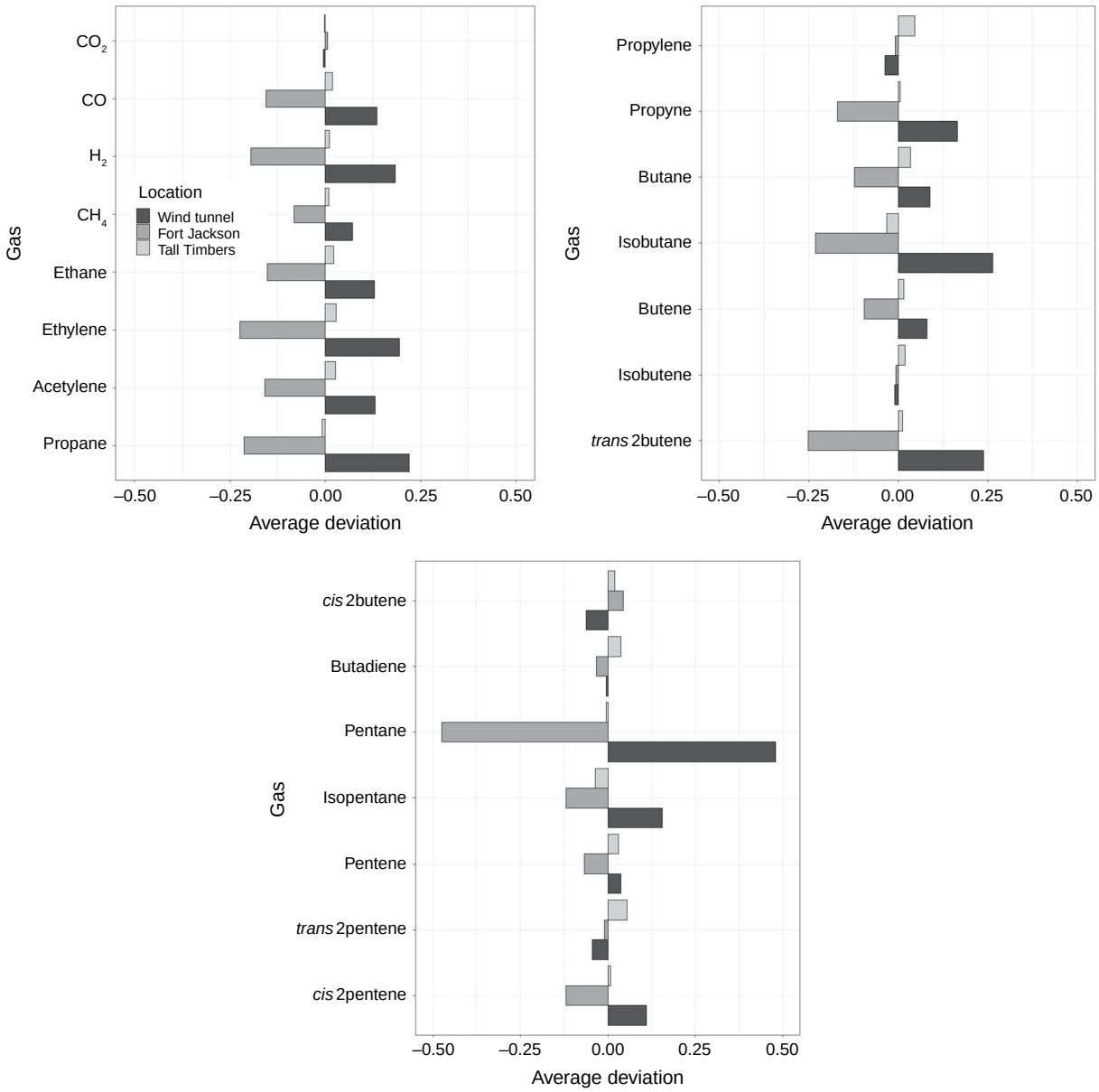

Fig. 4. Average deviation (log-ratio scale) from the mean by location for pyrolysis gases collected in a wind tunnel or in prescribed burns in longleaf pine fuel beds in the southeastern US.

and 16 polycyclic aromatic hydrocarbons (Bignal *et al.* 2008). In this study, wood chips were used instead of intact wildland fuels burned under open burning conditions; CO again was the only common gas. Similarly, the only gases in common with Possell and Bell (2013) were CO and CO_2.

The second challenge is that no studies have treated fire emissions as compositional data to date; thus, any sort of result based on the use of correlation (which includes regression) is subject to 'spurious correlation' (Aitchison 1986). Comparison of our results with other published data required applying the same analysis techniques to the published data. This was done for a single study (Tihay-Felicelli *et al.* 2017) (denoted TF). The TF study reported gas measurements sampled during the burning of piles of *Cistus monspeliensis* L., a common shrub of the Mediterranean region. Fuel loading (three levels) and moisture content (three levels) were controlled. Mean emission factors were presented for 16 gases; of these, CO, CO_2, CH_4, C_2H_2, C_2H_4, C_3H_6, C_3H_8 and C_4H_6 were common to both studies. A generic *ilr* transformation was applied to the TF data. Because the TF data set only contained nine observations and regular multivariate analysis of variance required more than 16 observations, a distribution-free permutation approach was used to test the significance of fuel moisture and loading (Anderson 2017). This analysis confirmed that fuel loading and moisture content significantly affected the composition of the TF gases.

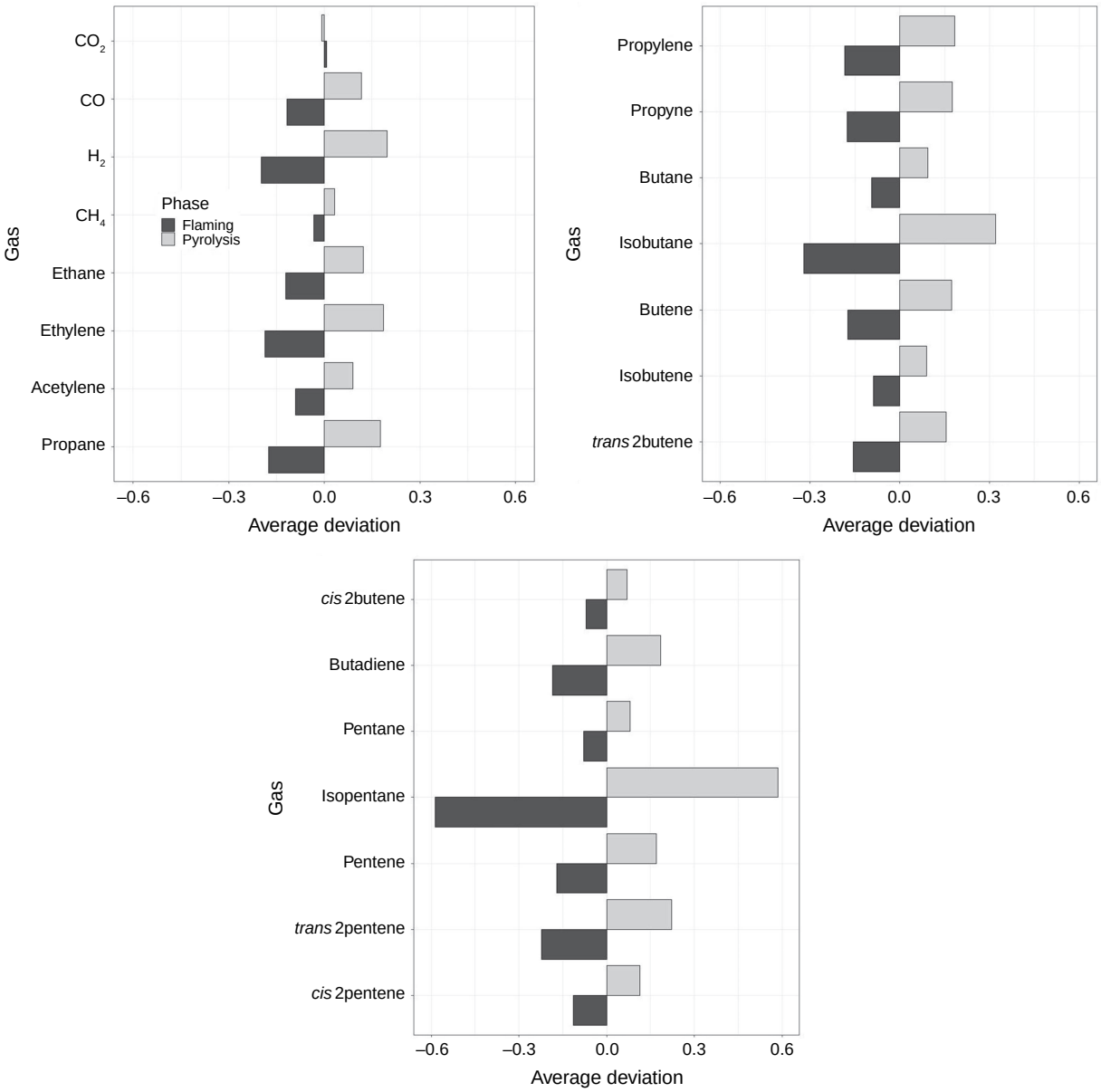

Fig. 5. Average deviation (log-ratio scale) from the mean by fire phase for pyrolysis gases collected in a wind tunnel or in prescribed burns in longleaf pine fuel beds in the southeastern US.

The same permutation approach applied to data extracted from fig. 3 of Xiong *et al.* (2013) produced mixed results. The gas composition was related to moisture content using linear regression; the logarithm of moisture content (appropriate for a ratio scale variable; van den Boogaart and Tolosana-Delgado 2013) was not significant whereas moisture content significantly affected the *ilr* coordinates. The permutation approach applied to Commandré *et al.* (2011) who studied pine wood with a moisture content of 10.7%, a value close to the fuel moisture of the pine needles in the present experiment, found that moisture content did not affect the composition of the six gases measured. Evans and Milne (1987) suggested that moisture content of biomass fuel had only a secondary effect on biomass oil composition from ponderosa pine (*P. ponderosa* Lawson & C. Lawson) wood even though its impact on yield could be appreciable. Although there may be consensus in the literature that moisture content affects the yield of pyrolysis products from biomass, the effect on gas composition is not settled as these analyses show. The fuels and configurations all differ from the approach in the present study, which complicates the ability to compare the present results with the literature.

Gas composition also differed between the wind tunnel and field samples from prescribed burns. While the overstorey at both field locations was dominated by longleaf

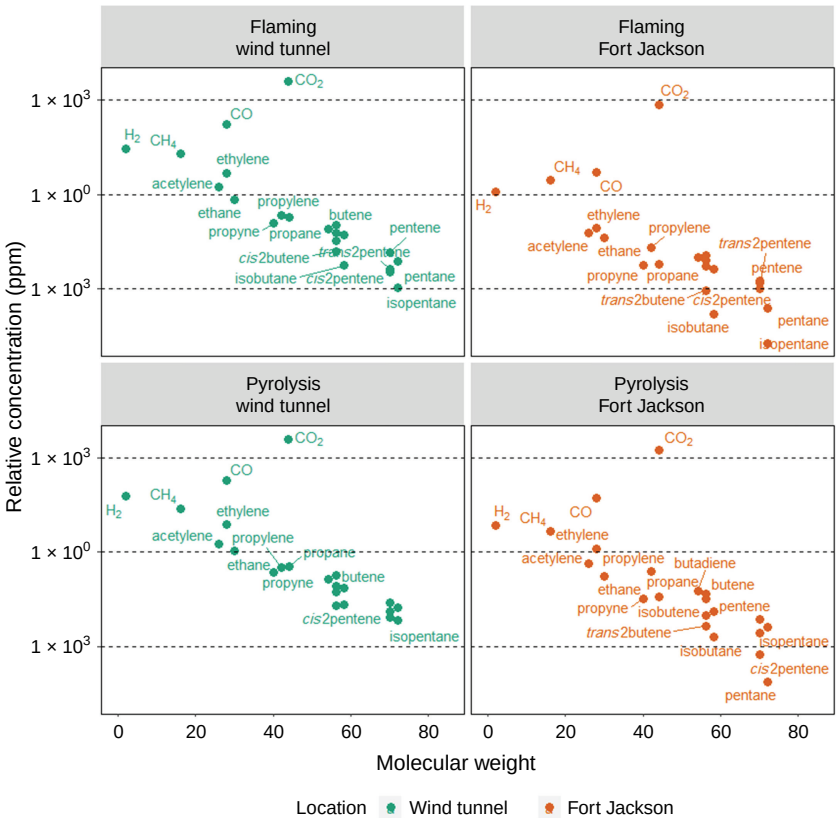

Fig. 6. Observed relative concentration of gases from pyrolysis and flaming combustion in wind tunnel and field burns in longleaf pine fuel beds.

Table 3. Pairwise comparisons of location and fire phase effects on selected balance values for gases. Effects that did not differ are indicated by the same letter with the letter values ordered from smallest to largest value. *P*-values adjusted to control for false discovery rate at 0.05 (Benjamini and Hochberg 1995).

Balance[A]	Location			Phase	
	Wind tunnel	Fort Jackson	Tall Timbers	Flaming	Pyrolysis
Zhou vs NMOC	13.9a	14.3a	13.7a	14.4b	13.7a
H_2 vs CO_2, CO, CH_4	3.7a	4.6b	3.5a	4.1b	3.6a
CO_2 vs CO, CH_4	−0.3b	−0.7a	−0.5ab	−0.6a	−0.2b
CO vs CH_4	1.5a	1.1a	1.6a	1.3a	1.5a
Alkanes vs other NMOC	−1.5b	−3.4a	−3.4ab	−2.3a	−1.7a
Alkenes vs alkynes	−2.5a	−2.1a	−2.3a	−2.4a	−2.4a

[A]See Table 1.

pine, the understorey composition differed. Owing to sampling design, any differences due to vegetation at Tall Timbers and Fort Jackson were confounded with all other site variables.

The consistent results showing that the relative concentrations of all gases except CO_2 were greater in the pyrolysis samples compared with the flaming samples were not surprising. The proportion of the total amount of gas pyrolysed that was sampled in the wind tunnel and in the field is unknown. Flaming samples in the wind tunnel were collected from the flame at approximately midflame height in a very turbulent environment. Pyrolysis gas sampling in the wind tunnel prior to flame arrival and at the base of the flame in the field may not be equivalent sampling locations. Such an effect – gas sampling location was confounded with experiment location interacting with the fire phase – would be contained in the fire phase–location interaction term, which was significant though not shown in Appendix Table A7. The temperature of the sampled gases was unknown; however, they were extracted near the base of the flame so should have been of the same order of magnitude. We have no reason to suspect that the sampling apparatus affected the composition

as very similar equipment was used in the wind tunnel and field (suction pump, metal tubing, etc.).

The field samples, while different in some manner from the wind tunnel samples, were successfully categorised into flaming and pyrolysis samples using a model developed from the measured composition of wind tunnel gas samples. Water vapour is a key component of gas produced by wildland fire (e.g. Scharko *et al.* 2019*b*), and studies have shown that H_2O is still present in the foliage of living plants even as ignition is occurring (Fletcher *et al.* 2007; Yashwanth *et al.* 2016). The canister samples were processed in such a manner that the water vapour was not accounted for. Other concurrent measurements of the gases using FTIR and quantum cascade lasers (Phillips *et al.* 2020) quantified the amount of H_2O. Inclusion of H_2O in the composition will not affect the results of the present analysis due to the *ilr*-coordinate approach we used. However, H_2O measurement may account for the relative difference in H_2 concentrations noted between the pyrolysis and flaming combustion samples. An analysis of variance comparing the present results with a subcomposition (CO, CO_2, CH_4, C_2H_2, C_2H_4) of smoke measured from similar prescribed burns at Fort Jackson in 2011 (Akagi *et al.* 2014) using an open-path FTIR indicated that the composition of both the pyrolysis and flaming samples differed from the 2011 measurements. The cause for the difference is unknown; the understorey was slightly different, the sampling locations (2011 – smoke drifting past the sensor, 2018 – intentional placement of sampling probe), the instruments used (FTIR vs GC/MS) and the number of samples (34 vs 3) differed. Comparison of both the wind tunnel flaming and pyrolysis subcompositions containing CO, CO_2, CH_4, C_2H_2, C_2H_4 and C_3H_6 with smoke samples from air-dried fuels burned in the Forest Service's Missoula Fire Sciences Lab (Burling *et al.* 2010; Hosseini *et al.* 2013) found that the compositions differed. The cause of the difference cannot be determined as different measurement methods (Missoula-FTIR) and fuel beds were used. It is important to note that, while the Missoula fuel beds from the southeastern US contained live plant material, the moisture content of the live component was much lower (maximum 31.5%) than the live fuels in the present study. Confirmation of the differences in composition of the pyrolysis samples, lab and field-based measurements of smoke (primarily from flaming combustion) provides further support for the conclusion that a composition of pyrolysis gases has been successfully measured in a field setting.

Urbanski *et al.* (2008) compiled smoke emissions data from prescribed burns collected using the FASS in a wide variety of southeastern US fuel types that were described in general terms. We compared the subcomposition containing CO, CO_2, CH_4, C_2H_2, C_2H_4, C_2H_6, C_3H_4, C_3H_6 and C_3H_8 for the Fort Jackson flaming samples and all southeastern fuel types using analysis of variance, which indicated that the Fort Jackson samples differed from the Urbanski data. Since H_2 was not reported, the two balances in Table 1 containing H_2 were not available; the log-ratio of the remaining dominant gases (CO, CO_2 and CH_4) with the NMOC were compared. Urbanski *et al.* (2008) reported that alkenes dominated their corresponding alkanes. In our comparison, the log-ratio for the dominant gases vs NMOC was larger at Fort Jackson; relatively more CO vs CH_4 and more alkenes than alkanes or alkynes were observed by Urbanski. The log-ratio of CO_2 with CO and CH_4 did not differ between the Fort Jackson and Urbanski data sets for flaming combustion. Although this last comparison supports the methodology used in the present study, it is important to note that the results are based on different fuel types, different sampling equipment, different burning conditions, etc. and only flaming combustion. We have been unable to locate other experiments in which pyrolysis samples were collected under similar settings. Statistical approaches linking lab and field emissions data using the carbon mass balance method (Ward *et al.* 1979; Nelson 1982; Radke *et al.* 1990; Yokelson *et al.* 1999) and modified combustion efficiency (MCE, Ward and Hao 1991) have been used (e.g. Yokelson *et al.* 2013); however, these approaches have recently faced criticism both from a statistical perspective (Weise *et al.* 2020*b*) and a technical perspective (Surawski *et al.* 2016).

It is well known that the pyrolysis of lignocellulosic fuels is affected by many factors including heating rate, fuel composition, fuel physical properties, temperature and atmosphere to mention some. It is a premise of experimental design that controlling the variation of as many factors as is feasible permits hypothesis testing in order to identify relationships between the controlled factors and the response variable (Mason *et al.* 1989). In the present study, every effort was made to control the natural variability of fuel composition and physical properties and heating rate in the design while using a repeatable sampling technique and standard analysis techniques and measuring other variables such as air temperature and atmospheric humidity that might be correlated with gas composition in order to determine differences in pyrolysis gases. Even with this level of control of a fire experiment, there are unmeasured variables that may be also important beyond what was identified in the planning of the experiments. Regardless of these limitations in the data, this study was able to demonstrate that it is possible to measure wildland fuel pyrolysis under conditions less controlled than those described by Dimitrakopoulos (2001) in order to improve our ability to model wildland fires chemically and physically. This study can provide a first step to the chemical measurement of the fire phenomenon in realistic settings.

Conclusions

Overall, CO_2 was the dominant gas observed in canister samples collected in both a laboratory setting in a wind tunnel and from wildland fire flames measured during operational

prescribed burns in longleaf pine. Other dominant gases included CO, H_2, and CH_4 based on relative amounts. Although the relative amounts of CO, CO_2, and CH_4 were similar between fire phases (pyrolysis, flaming combustion), relatively more H_2 was observed in the pyrolysis canisters. For the other 21 measured gases, log-ratios with CO_2 were consistently larger in the pyrolysis samples, indicating either more of the gas was released or less CO_2 was produced. Fire phase affected the gas composition significantly. Air temperature was varied to simulate growing and dormant (winter) season conditions and did not significantly affect the composition of the wind tunnel samples. The presence of live plants in the wind tunnel experiment significantly affected gas composition. Several fuel bed types affected the relative amounts of individual gases similarly.

Logistic regression correctly classified 76% of the wind tunnel samples as flaming combustion or pyrolysis. Application of this model to the field data predicted that 60% of the field samples were from pyrolysis. Comparison of the wind tunnel samples with the field samples found that location (wind tunnel, field) and fire phase affected composition of the gas samples. Use of compositional data analysis enabled the use of common statistical methods to analyse gas composition and produce results consistent with the nature of the data.

Supplementary material

Supplementary material is available online.

References

Aitchison J (1986) 'The statistical analysis of compositional data.' (Chapman and Hall: London; New York, NY)

Akagi SK, Burling IR, Mendoza A, Johnson TJ, Cameron M, Griffith DWT, Paton-Walsh C, Weise DR, Reardon J, Yokelson RJ (2014) Field measurements of trace gases emitted by prescribed fires in southeastern US pine forests using an open-path FTIR system. *Atmospheric Chemistry and Physics* **14**, 199–215. doi:10.5194/acp-14-199-2014

Alexander ME, Cruz MG (2011) Interdependencies between flame length and fireline intensity in predicting crown fire initiation and crown scorch height. *International Journal of Wildland Fire* **21**, 95–113. doi:10.1071/WF11001

Aminfar A (2019) Application of computer vision to transport phenomena. PhD dissertation. University of California, Riverside.

Aminfar A, Cobian-Iñiguez J, Ghasemian M, Rosales Espitia N, Weise DR, Princevac M (2020) Using background-oriented schlieren to visualize convection in a propagating wildland fire. *Combustion Science and Technology* **192**, 2259–2279. doi:10.1080/00102202.2019.1635122

Amini E, Safdari M-S, DeYoung JT, Weise DR, Fletcher TH (2019*a*) Characterization of pyrolysis products from slow pyrolysis of live and dead vegetation native to the southern United States. *Fuel* **235**, 1475–1491. doi:10.1016/j.fuel.2018.08.112

Amini E, Safdari M-S, Weise DR, Fletcher TH (2019*b*) Pyrolysis kinetics of live and dead wildland vegetation from the southern United States. *Journal of Analytical and Applied Pyrolysis* **142**, 104613. doi:10.1016/j.jaap.2019.05.002

Amini E, Safdari M-S, Johnson N, Weise DR, Fletcher TH (2021) Pyrolysis kinetics of wildland vegetation using model-fitting methods. *Journal of Analytical and Applied Pyrolysis* **157**, 105167. doi:10.1016/j.jaap.2021.105167

Andersen J, Rasmussen CL, Giselsson T, Glarborg P (2009) Global combustion mechanisms for use in CFD modeling under oxy-fuel conditions. *Energy & Fuels* **23**, 1379–1389. doi:10.1021/ef8003619

Anderson HE, Rothermel RC (1965) Influence of moisture and wind upon the characteristics of free-burning fires. *Symposium (International) on Combustion* **10**, 1009–1019. doi:10.1016/S0082-0784(65)80243-0

Anderson MJ (2017) Permutational Multivariate Analysis of Variance (PERMANOVA). In 'Wiley StatsRef: Statistics Reference Online'. (Eds N Balakrishnan, T Colton, B Everitt, W Piegorsch, F Ruggeri, JL Teugels) pp. 1–15. (John Wiley & Sons, Ltd: Chichester, UK) doi:10.1002/9781118445112.stat07841

Antal MJ (1985*a*) Biomass pyrolysis: a review of the literature Part 1 – carbohydrate pyrolysis. In 'Advances in Solar Energy: An Annual Review of Research and Development, Volume 1 '. (Eds KW Böer, JA Duffie) pp. 61–111. (Springer New York: Boston, MA) doi:10.1007/978-1-4684-8992-7_3

Antal MJ (1985*b*) Biomass pyrolysis: a review of the literature part 2 – lignocellulose pyrolysis. In 'Advances in Solar Energy: An Annual Review of Research and Development Volume 2'. (Eds KW Böer, JA Duffie) pp. 175–255. (Springer US: Boston, MA) doi:10.1007/978-1-4613-9951-3_4

ASTM International (2016) ASTM D4442–16. Standard Test Methods for Direct Moisture Content Measurement of Wood and Wood-Base Materials. Available at https://www.astm.org/Standards/D4442.htm

Austin CC, Wang D, Ecobichon DJ, Dussault G (2001) Characterization of volatile organic compounds in smoke at experimental fires. *Journal of Toxicology and Environmental Health, Part A* **63**, 191–206. doi:10.1080/15287390151101547

Banach CA, Bradley AM, Tonkyn RG, Williams ON, Chong J, Weise DR, Myers TL, Johnson TJ (2021) Dynamic infrared gas analysis from longleaf pine fuel beds burned in a wind tunnel: observation of phenol in pyrolysis and combustion phases. *Atmospheric Measurement Techniques* **14**, 2359–2376. doi:10.5194/amt-14-2359-2021

Bartoli P, Simeoni A, Biteau H, Torero JL, Santoni PA (2011) Determination of the main parameters influencing forest fuel combustion dynamics. *Fire Safety Journal* **46**, 27–33. doi:10.1016/j.firesaf.2010.05.002

Bartolome C, Princevac M, Weise DR, Mahalingam S, Ghasemian M, Venkatram A, Vu H, Aguilar G (2019) Laboratory and numerical modeling of the formation of superfog from wildland fires. *Fire Safety Journal* **106**, 94–104. doi:10.1016/j.firesaf.2019.04.009

Bates D, Mächler M, Bolker B, Walker S (2015) Fitting linear mixed-effects models using lme4. *Journal of Statistical Software* **67**, 1–48. doi:10.18637/jss.v067.i01

Benjamini Y, Hochberg Y (1995) Controlling the false discovery rate: a practical and powerful approach to multiple testing. *Journal of the Royal Statistical Society Series B (Methodological)* **57**, 289–300. doi:10.1111/j.2517-6161.1995.tb02031.x

Bignal KL, Langridge S, Zhou JL (2008) Release of polycyclic aromatic hydrocarbons, carbon monoxide and particulate matter from biomass combustion in a wood-fired boiler under varying boiler conditions. *Atmospheric Environment* **42**, 8863–8871. doi:10.1016/j.atmosenv.2008.09.013

Borujerdi PR (2021) Physics-based modeling of pyrolysis and combustion of live leaves in wildfires. PhD dissertation, University of Alabama in Huntsville, Huntsville, AL. 179 p.

Bracewell JM (1971) Characterization of soils by pyrolysis combined with mass spectrometry. *Geoderma* **6**, 163–168. doi:10.1016/0016-7061(71)90003-6

Bretz F, Hothorn T, Westfall PH (2011) 'Multiple comparisons using R.' (CRC Press: Boca Raton, FL)

Broido A (1968) On the Chatterjee method of obtaining kinetic parameters from thermogravimetric traces. *Journal of Polymer Science Part B: Polymer Letters* **6**, 349–351. doi:10.1002/pol.1968.110060506

Broido A, Kilzer FJ (1963) A critique of the present state of knowledge of the mechanism of cellulose pyrolysis. *Fire Research Abstracts and Reviews* **5**, 157–161.

Buessing L, Goldfarb JL (2012) Energy along Interstate I-95: pyrolysis kinetics of Floridian cabbage palm (Sabal palmetto). *Journal of Analytical and Applied Pyrolysis* **96**, 78–85. doi:10.1016/j.jaap.2012.03.008

Burling IR, Yokelson RJ, Griffith DWT, Johnson TJ, Veres P, Roberts JM, Warneke C, Urbanski SP, Reardon J, Weise DR, Hao WM, de Gouw J (2010) Laboratory measurements of trace gas emissions from

biomass burning of fuel types from the southeastern and southwestern United States. *Atmospheric Chemistry and Physics* **10**, 11115–11130. doi:10.5194/acp-10-11115-2010

Butler B, Teske C, Jimenez D, O'Brien J, Sopko P, Wold C, Vosburgh M, Hornsby B, Loudermilk E (2016) Observations of energy transport and rate of spreads from low-intensity fires in longleaf pine habitat – RxCADRE 2012. *International Journal of Wildland Fire* **25**, 76–89. doi:10.1071/WF14154

Butler BM, Palarea-Albaladejo J, Shepherd KD, Nyambura KM, Towett EK, Sila AM, Hillier S (2020) Mineral–nutrient relationships in African soils assessed using cluster analysis of X-ray powder diffraction patterns and compositional methods. *Geoderma* **375**, 114474. doi:10.1016/j.geoderma.2020.114474

Butler BW, Cohen J, Latham DJ, Schuette RD, Sopko P, Shannon KS, Jimenez D, Bradshaw LS (2004) Measurements of radiant emissive power and temperatures in crown fires. *Canadian Journal of Forest Research* **34**, 1577–1587. doi:10.1139/x04-060

Byram GM (1959) Combustion of forest fuels. In 'Forest Fire: Control and Use'. (Ed. KP Davis) pp. 61–89. (McGraw-Hill: New York, NY)

Cancellieri D, Leoni E, Rossi JL (2005) Kinetics of the thermal degradation of *Erica arborea* by DSC: hybrid kinetic method. *Thermochimica Acta* **438**, 41–50. doi:10.1016/j.tca.2005.07.013

Chen L-WA, Verburg P, Shackelford A, Zhu D, Susfalk R, Chow JC, Watson JG (2010) Moisture effects on carbon and nitrogen emission from burning of wildland biomass. *Atmospheric Chemistry and Physics* **10**, 6617–6625. doi:10.5194/acp-10-6617-2010

Chetehouna K, Barboni T, Zarguili I, Leoni E, Simeoni A, Fernandez-Pello AC (2009) Investigation on the emission of volatile organic compounds from heated vegetation and their potential to cause an accelerating forest fire. *Combustion Science and Technology* **181**, 1273–1288. doi:10.1080/00102200903181827

Chetehouna K, Courty L, Lemée L, Garo JP, Gillard P (2012) Experimental determination of volatile organic compounds emitted by *Thymus vulgaris*. *WIT Transactions on Ecology and the Environment* **158**, 189–198doi:10.2495/FIVA120161

Chetehouna K, Courty L, Mounaïm-Rousselle C, Halter F, Garo J-P (2013) Combustion characteristics of *p*-cymene possibly involved in accelerating forest fires. *Combustion Science and Technology* **185**, 1295–1305. doi:10.1080/00102202.2013.795557

Clark MM, Fletcher TH, Linn RR (2010) A sub-grid, mixture fraction-based thermodynamic equilibrium model for gas phase combustion in FIRETEC: development and results. *International Journal of Wildland Fire* **19**, 202–212. doi:10.1071/WF07116

Cohen JD (2015) Fuel particle heat exchange during wildland fire spread. PhD Thesis, University of Idaho, Moscow, Idaho.

Collard F-X, Blin J (2014) A review on pyrolysis of biomass constituents: mechanisms and composition of the products obtained from the conversion of cellulose, hemicelluloses and lignin. *Renewable and Sustainable Energy Reviews* **38**, 594–608. doi:10.1016/j.rser.2014.06.013

Commandré J-M, Lahmidi H, Salvador S, Dupassieux N (2011) Pyrolysis of wood at high temperature: The influence of experimental parameters on gaseous products. *Fuel Processing Technology* **92**, 837–844. doi:10.1016/j.fuproc.2010.07.009

Costa VJ, Vieira RM, Girotto S, Simioni FJ (2016) Pyrolysis and thermogravimetry of blended and nonblended residues of pine and eucalyptus forestry woods. *Environmental Progress & Sustainable Energy* **35**, 1521–1528. doi:10.1002/ep.12372

Di Blasi C (2008) Modeling chemical and physical processes of wood and biomass pyrolysis. *Progress in Energy and Combustion Science* **34**, 47–90. doi:10.1016/j.pecs.2006.12.001

Dietenberger MA, Boardman CR, Weise DR (2020) New methods for pyrolysis and combustion properties of forest litter: enhanced cone calorimetry with longleaf pine needles. In 'Proceedings of the Fire Continuum Conference'. (Eds SM Hood, S Drury, T Steelman, R Steffens) Proceedings. pp. 72–83. (USDA Forest Service Rocky Mountain Research Station: Fort Collins, CO). Available at https://www.fs.usda.gov/treesearch/pubs/60630

Dimitrakopoulos AP (2001) Thermogravimetric analysis of Mediterranean plant species. *Journal of Analytical and Applied Pyrolysis* **60**, 123–130. doi:10.1016/S0165-2370(00)00164-9

Dryer FL, Glassman I (1973) High-temperature oxidation of CO and CH4. *Fourteenth Symposium (International) on Combustion* **14**, 987–1003. doi:10.1016/S0082-0784(73)80090-6

Duvvuri M, Muhlenkamp S, Iqbal K, Welker J (1975) The pyrolysis of natural fuels. *Journal of Fire and Flammability* **6**, 468–477.

Egozcue JJ, Pawlowsky-Glahn V (2005) Groups of parts and their balances in compositional data analysis. *Mathematical Geology* **37**, 795–828. doi:10.1007/s11004-005-7381-9

Egozcue JJ, Pawlowsky-Glahn V, Mateu-Figueras G, Barceló-Vidal C (2003) Isometric logratio transformations for compositional data analysis. *Mathematical Geology* **35**, 279–300. doi:10.1023/A:1023818214614

El Houssami M, Thomas JC, Lamorlette A, Morvan D, Chaos M, Hadden R, Simeoni A (2016) Experimental and numerical studies characterizing the burning dynamics of wildland fuels. *Combustion and Flame* **168**, 113–126. doi:10.1016/j.combustflame.2016.04.004

EPA (1999) 'Compendium Method TO-14A Determination Of Volatile Organic Compounds (VOCs) In Ambient Air Using Specially Prepared Canisters With Subsequent Analysis By Gas Chromatography. Compendium of Methods for the Determination of Toxic Organic Compounds in Ambient Air'. p. 86. (Environmental Protection Agency: Cincinnati, OH). Available at https://www.epa.gov/sites/production/files/2019-11/documents/to-14ar.pdf

Evans JC, Huckaby JL, Mitroshkov AV, Julya JL, Hayes JC, Edwards JA, Sasaki LM (1998) 32-week holding-time study of SUMMA polished canisters and triple sorbent traps used to sample organic constituents in radioactive waste tank vapor headspace. *Environmental Science & Technology* **32**, 3410–3417. doi:10.1021/es9803153

Evans RJ, Milne TA (1987) Molecular characterization of the pyrolysis of biomass. *Energy & Fuels* **1**, 123–137. doi:10.1021/ef00002a001

Finney MA, Cohen JD, Forthofer JM, McAllister SS, Gollner MJ, Gorham DJ, Saito K, Akafuah NK, Adam BA, English JD (2015) Role of buoyant flame dynamics in wildfire spread. *Proceedings of the National Academy of Sciences* **112**(32), 9833–9838. doi:10.1073/pnas.1504498112

Fletcher TH, Pickett BM, Smith SG, Spittle GS, Woodhouse MM, Haake E, Weise DR (2007) Effects of moisture on ignition behavior of moist California chaparral and Utah leaves. *Combustion Science and Technology* **179**, 1183–1203. doi:10.1080/00102200601015574

Fons WL, Clements HB, George PM (1963) Scale effects on propagation rate of laboratory crib fires. *Symposium (International) on Combustion* **9**, 860–866. doi:10.1016/S0082-0784(63)80092-2

Font R, Conesa JA, Moltó J, Muñoz M (2009) Kinetics of pyrolysis and combustion of pine needles and cones. *Journal of Analytical and Applied Pyrolysis* **85**, 276–286. doi:10.1016/j.jaap.2008.11.015

Garofalo LA, Pothier MA, Levin EJT, Campos T, Kreidenweis SM, Farmer DK (2019) Emission and evolution of submicron organic aerosol in smoke from wildfires in the western United States. *ACS Earth and Space Chemistry* **3**, 1237–1247. doi:10.1021/acsearthspacechem.9b00125

Glueckauf E, Kitt GP (1957) The hydrogen content of atmospheric air at ground level. *Quarterly Journal of the Royal Meteorological Society* **83**, 522–528. doi:10.1002/qj.49708335808

Grishin AM (1997) 'Mathematical Modelling of Forest Fires and New Methods of Fighting Them'. (Ed. FA Albini) (Publishing House of Tomsk State University, Tomsk: Russia)

Haase SM, Sánchez JJ, Weise DR (2016) Evaluation of standard methods for collecting and processing fuel moisture samples. USDA Forest Service, Pacific Southwest Research Station, Research Paper PSW-RP-268. (Albany, CA). Available at http://www.treesearch.fs.fed.us/pubs/52252

Hadden RM, Rein G, Belcher CM (2013) Study of the competing chemical reactions in the initiation and spread of smouldering combustion in peat. *Proceedings of the Combustion Institute* **34**, 2547–2553. doi:10.1016/j.proci.2012.05.060

Hosseini S, Urbanski SP, Dixit P, Qi L, Burling IR, Yokelson RJ, Johnson TJ, Shrivastava M, Jung HS, Weise DR, Miller JW, Cocker DR (2013) Laboratory characterization of PM emissions from combustion of wildland biomass fuels: particle emissions from biomass burning. *Journal of Geophysical Research: Atmospheres* **118**, 9914–9929. doi:10.1002/jgrd.50481

Hothorn T, Bretz F, Westfall P (2008) Simultaneous inference in general parametric models. *Biometrical Journal* **50**, 346–363. doi:10.1002/bimj.200810425

Hough WA, Albini FA (1978) Predicting fire behavior in palmetto–gallberry fuel complexes. USDA Forest Service, Southeastern Forest

Experiment Station, Research Paper SE-174. (Asheville, NC). Available at https://www.srs.fs.usda.gov/pubs/rp/rp_se174.pdf
Hudak AT, Kato A, Bright BC, Loudermilk EL, Hawley C, Restaino JC, Ottmar RD, Prata GA, Cabo C, Prichard SJ, Rowell EM, Weise DR (2020) Towards spatially explicit quantification of pre- and postfire fuels and fuel consumption from traditional and point cloud measurements. *Forest Science* **66**, 428–442. doi:10.1093/forsci/fxz085
Huggett C (1984) Heating rates in fire experiments. *Journal of Fire Sciences* **2**, 257–259. doi:10.1177/073490418400200401
Jarvis TD (1995) Smokey science meets ecosystem management: a vision of the future. In 'Proceedings: Symposium on Fire in Wilderness and Park Management', Ogden, UT. General Technical Report. 137–138. (USDA Forest Service, Intermountain Research Station: Ogden, UT). Available at https://archive.org/details/CAT10714714/mode/2up
Johansen RW (1987) Ignition patterns & prescribed fire behavior in southern pine stands. Georgia Forestry Commission, Georgia Forest Research Paper 72. (Macon, GA). Available at http://www.treesearch.fs.fed.us/pubs/36482
Jordan A, Steinberg B (2011) Calibration of atmospheric hydrogen measurements. *Atmospheric Measurement Techniques* **4**, 509–521. doi:10.5194/amt-4-509-2011
Kan T, Strezov V, Evans TJ (2016) Lignocellulosic biomass pyrolysis: A review of product properties and effects of pyrolysis parameters. *Renewable and Sustainable Energy Reviews* **57**, 1126–1140. doi:10.1016/j.rser.2015.12.185
Kane JM, Varner JM, Knapp EE (2009) Novel fuelbed characteristics associated with mechanical mastication treatments in northern California and south-western Oregon, USA. *International Journal of Wildland Fire* **18**, 686. doi:10.1071/WF08072
Knapp EE, Varner JM, Busse MD, Skinner CN, Shestak CJ (2011) Behaviour and effects of prescribed fire in masticated fuelbeds. *International Journal of Wildland Fire* **20**, 932–945. doi:10.1071/WF10110
Korobeinichev OP, Paletsky AA, Gonchikzhapov MB, Shundrina IK, Chen H, Liu N (2013) Combustion chemistry and decomposition kinetics of forest fuels. *Procedia Engineering* **62**, 182–193. doi:10.1016/j.proeng.2013.08.054
Kreye JK, Kobziar LN (2015) The effect of mastication on surface fire behaviour, fuels consumption and tree mortality in pine flatwoods of Florida, USA. *International Journal of Wildland Fire* **24**, 573. doi:10.1071/WF14186
Kuznetsova A, Brockhoff PB, Christensen RHB (2017) lmerTest package: tests in linear mixed effects models. *Journal of Statistical Software* **82**, 1–26. doi:10.18637/jss.v082.i13
Lautenberger C (2014) Gpyro3D: a three dimensional generalized pyrolysis model. *Fire Safety Science* **11**, 193–207. doi:10.3801/IAFSS.FSS.11-193
Lautenberger C, Fernandez-Pello C (2009) Generalized pyrolysis model for combustible solids. *Fire Safety Journal* **44**, 819–839. doi:10.1016/j.firesaf.2009.03.011
Leroy V, Leoni E, Santoni P-A (2008) Reduced mechanism for the combustion of evolved gases in forest fires. *Combustion and Flame* **154**, 410–433. doi:10.1016/j.combustflame.2008.04.014
Liodakis S, Bakirtzis D, Dimitrakopoulos A (2002) Ignition characteristics of forest species in relation to thermal analysis data. *Thermochimica Acta* **390**, 83–91. doi:10.1016/S0040-6031(02)00077-1
Lyon ZD, Morgan P, Stevens-Rumann CS, Sparks AM, Keefe RF, Smith AMS (2018) Fire behaviour in masticated forest fuels: lab and prescribed fire experiments. *International Journal of Wildland Fire* **27**, 280. doi:10.1071/WF17145
Martin RE, Davis LS (1961) Temperatures near the ground during prescribed burning. *Papers of the Michigan Academy of Science, Arts, and Letters* **46**, 239–249.
Mason RL, Gunst RF, Hess JL (1989) 'Statistical design and analysis of experiments: with applications to engineering and science.' (Wiley: New York). Available at https://www.cs.ubc.ca/~hutter/EARG.shtml/earg/papers05/Stat_Analysis_of_Exp_Gunst_Hess.pdf
Matt FJ, Dietenberger MA, Weise DR (2020) Summative and ultimate analysis of live leaves from southern US forest plants for use in fire modeling. *Energy & Fuels* **34**, 4703–4720. doi:10.1021/acs.energyfuels.9b04107
McCullagh P, Nelder JA (1998) 'Generalized linear models.' (Chapman & Hall/CRC: Boca Raton)
Mell W, Maranghides A, McDermott R, Manzello SL (2009) Numerical simulation and experiments of burning douglas fir trees. *Combustion and Flame* **156**, 2023–2041. doi:10.1016/j.combustflame.2009.06.015
Moghtaderi B (2006) The state-of-the-art in pyrolysis modelling of lignocellulosic solid fuels. *Fire and Materials* **30**, 1–34. doi:10.1002/fam.891
Montero-Serrano JC, Palarea-Albaladejo J, Martín-Fernández JA, Martínez-Santana M, Gutiérrez-Martín JV (2010) Sedimentary chemofacies characterization by means of multivariate analysis. *Sedimentary Geology* **228**, 218–228. doi:10.1016/j.sedgeo.2010.04.013
Montgomery RR, Crivellone MD (Eds) (2021) 'SRM NIST Standard Reference Materials Catalog.' Special Publication (NIST SP) (National Institute of Standards and Technology: Gaithersburg, MD). Available at https://tsapps.nist.gov/publication/get_pdf.cfm?pub_id=931807
Morvan D, Dupuy JL (2004) Modeling the propagation of a wildfire through a Mediterranean shrub using a multiphase formulation. *Combustion and Flame* **138**, 199–210. doi:10.1016/j.combustflame.2004.05.001
Morvan D, Accary G, Meradji S, Frangieh N, Bessonov O (2018) A 3D physical model to study the behavior of vegetation fires at laboratory scale. *Fire Safety Journal* **101**, 39–52. doi:10.1016/j.firesaf.2018.08.011
Nelson Jr RM (1980) Flame characteristics for fires in southern fuels. USDA Forest Service, Southeastern Forest Experiment Station, Research Paper SE-RP-205. (Asheville, NC) https://doi.org/10.2737/SE-RP-205
Nelson Jr RM (1982) An evaluation of the carbon balance technique for estimating emission factors and fuel consumption in forest fire. USDA Forest Service, Southeastern Forest Experiment Station, Research Paper SE-231. (Asheville, NC) https://doi.org/10.2737/SE-RP-231
Nelson Jr RM, Butler BW, Weise DR (2012) Entrainment regimes and flame characteristics of wildland fires. *International Journal of Wildland Fire* **21**, 127–140. doi:10.1071/WF10034
Ostertag TE, Robertson KM (2007) A comparison of native versus old-field vegetation in upland pinelands managed with frequent fire, south Georgia, USA. In 'Proceedings of the 23rd Tall Timbers Fire Ecology Conference: Fire in Grassland & Shrubland Ecosystems', Tallahassee, FL. 109–120. (Eds RE Masters, KLM Galley) (Tall Timbers Research Station: Tallahassee, FL). Available at https://talltimbers.org/wp-content/uploads/2018/09/109-OstertagandRobertson2007.pdf
Ottmar RD, Andreu A (2007) Litter and duff bulk densities in the southern United States – final report to the Joint Fire Science Program. USDA Forest Service, Pacific Northwest Research Station, Final Report JFSP Project No. 04-2-1-49. (Seattle, WA). Available at https://www.firescience.gov/projects/04-2-1-49/project/04-2-1-49_final_report.pdf
Palarea-Albaladejo J, Martín-Fernández JA (2013) Values below detection limit in compositional chemical data. *Analytica Chimica Acta* **64** , 32–43. doi:10.1016/j.aca.2012.12.029
Palarea-Albaladejo J, Martín-Fernández JA (2015) zCompositions — R package for multivariate imputation of left-censored data under a compositional approach. *Chemometrics and Intelligent Laboratory Systems* **143**, 85–96. doi:10.1016/j.chemolab.2015.02.019
Pecha MB, Garcia-Perez M (2020) Pyrolysis of lignocellulosic biomass: oil, char, and gas. In 'Bioenergy'. (Ed. A Dahiya) pp. 581–619. (Elsevier) 10.1016/B978-0-12-815497-7.00029-4
Peet RK, Allard DJ (1993) Longleaf pine vegetation of the southern Atlantic and eastern Gulf Coast regions: a preliminary classification. In 'Proceedings of the Tall Timbers Fire Ecology Conference, No. 18, The Longleaf Pine Ecosystem: ecology, restoration and management'. (Ed SM Hermann) pp. 45–81. Tall Timbers Research Station, Tallahassee, FL. Available at https://talltimbers.org/wp-content/uploads/2018/09/45-PeetandAllard1993_op.pdf
Phillips MC, Myers TL, Johnson TJ, Weise DR (2020) In-situ measurement of pyrolysis and combustion gases from biomass burning using swept wavelength external cavity quantum cascade lasers. *Optics Express* **28**, 8680. doi:10.1364/OE.386072
Pinheiro JC, Bates DM (2000) 'Mixed-effects models in S and S-PLUS.' (Springer: New York, NY)
Possell M, Bell TL (2013) The influence of fuel moisture content on the combustion of Eucalyptus foliage. *International Journal of Wildland Fire* **22**, 343–352. doi:10.1071/WF12077
Radke LF, Lyons JH, Hobbs PV, Hegg DA, Sandberg DV, Ward DE (1990) Airborne monitoring and smoke characterization of

prescribed fires on forest lands in western Washington and Oregon. USDA Forest Service, Pacific Northwest Research Station, PNW-GTR-251. (Portland, OR) doi:10.2737/PNW-GTR-251.

Robertson K, Ostertag T (2007) Effects of land use on fuel characteristics and fire behavior in pinelands of southwest Georgia. In 'Proceedings of the 23rd Tall Timbers Fire Ecology Conference: Fire in Grassland & Shrubland Ecosystems', Tallahassee, FL. 181–191. (Eds RE Masters, KLM Galley) (Tall Timbers Research Station: Tallahassee, FL)

Rothermel RC (1972) A mathematical model for predicting fire spread in wildland fuels. USDA Forest Service, Intermountain Forest and Range Experiment Station, Research Paper INT-115. (Ogden, UT). Available at http://www.fs.fed.us/rm/pubs_int/int_rp115.pdf

Rothermel RC, Anderson HE (1966) Fire spread characteristics determined in the laboratory. USDA Forest Service, Intermountain Forest and Range Experiment Station, Research Paper INT-30. (Ogden, UT). Available at https://www.fs.fed.us/rm/pubs_int/int_rp030.pdf

Rothermel RC, Philpot CW (1973) Predicting changes in chaparral flammability. *Journal of Forestry* **1** , 640–643.

Roy C, Chornet E, Fuchsman CH (1983) The pyrolysis of peat. *Journal of Analytical and Applied Pyrolysis* **5**, 261–332. doi:10.1016/0165-2370(83)80033-3

Safdari M-S, Rahmati M, Amini E, Howarth JE, Berryhill JP, Dietenberger M, Weise DR, Fletcher TH (2018) Characterization of pyrolysis products from fast pyrolysis of live and dead vegetation native to the Southern United States. *Fuel* **229**, 151–166. doi:10.1016/j.fuel.2018.04.166

Safdari M-S, Amini E, Weise DR, Fletcher TH (2019) Heating rate and temperature effects on pyrolysis products from live wildland fuels. *Fuel* **242**, 295–304. doi:10.1016/j.fuel.2019.01.040

Safdari M-S, Amini E, Weise DR, Fletcher TH (2020) Comparison of pyrolysis of live wildland fuels heated by radiation vs convection. *Fuel* **268**, 117342. doi:10.1016/j.fuel.2020.117342

Scharko NK, Oeck AM, Myers TL, Tonkyn RG, Banach CA, Baker SP, Lincoln EN, Chong J, Corcoran BM, Burke GM, Ottmar RD, Restaino JC, Weise DR, Johnson TJ (2019*a*) Gas-phase pyrolysis products emitted by prescribed fires in pine forests with a shrub understory in the southeastern United States. *Atmospheric Chemistry and Physics* **19**, 9681–9698. doi:10.5194/acp-19-9681-2019

Scharko NK, Oeck AM, Tonkyn RG, Baker SP, Lincoln EN, Chong J, Corcoran BM, Burke GM, Weise DR, Myers TL, Banach CA, Griffith DWT, Johnson TJ (2019*b*) Identification of gas-phase pyrolysis products in a prescribed fire: first detections using infrared spectroscopy for naphthalene, methyl nitrite, allene, acrolein and acetaldehyde. *Atmospheric Measurement Techniques* **12**, 763–776. doi:10.5194/amt-12-763-2019

Schuette RD (1965) Preparing reproducible pine needle fuel beds. USDA Forest Service, Intermountain Forest and Range Experiment Station, Research Note INT-36. (Ogden, UT)

Shafizadeh F (1982) Introduction to the pyrolysis of biomass. *Journal of Analytical and Applied Pyrolysis* **3**, 283–305. doi:10.1016/0165-2370(82)80017-X

Shafizadeh F, Philpot CW, Ostojic N (1971) Thermal analysis of 1,6-anhydro-β-D-glucopyranose. *Carbohydrate Research* **16**, 279–287. doi:10.1016/S0008-6215(00)81162-3

Simpson IJ, Akagi SK, Barletta B, Blake NJ, Choi Y, Diskin GS, Fried A, Fuelberg HE, Meinardi S, Rowland FS, Vay SA, Weinheimer AJ, Wennberg PO, Wiebring P, Wisthaler A, Yang M, Yokelson RJ, Blake DR (2011) Boreal forest fire emissions in fresh Canadian smoke plumes: C_1-C_{10} volatile organic compounds (VOCs), CO_2, CO, NO_2, NO, HCN and CH_3CN. *Atmospheric Chemistry and Physics* **11**, 6445–6463. doi:10.5194/acp-11-6445-2011

Snyder EB, Hamaker JM (1978) Needle characteristics of hybrids of some species of southern pine. *Silvae Genetica* **27**, 184–188.

Statheropoulos M, Liodakis S, Tzamtzis N, Pappa A, Kyriakou S (1997) Thermal degradation of *Pinus halepensis* pine-needles using various analytical methods. *Journal of Analytical and Applied Pyrolysis* **43**, 115–123. doi:10.1016/S0165-2370(97)00064-8

Strand T, Gullett B, Urbanski S, O'Neill S, Potter B, Aurell J, Holder A, Larkin N, Moore M, Rorig M (2016) Grassland and forest understorey biomass emissions from prescribed fires in the south-eastern United States – RxCADRE 2012. *International Journal of Wildland Fire* **25**, 102–113. doi:10.1071/WF14166

Surawski NC, Sullivan AL, Roxburgh SH, Meyer CPM, Polglase PJ (2016) Incorrect interpretation of carbon mass balance biases global vegetation fire emission estimates. *Nature Communications* , 11536. doi:10.1038/ncomms11536

Susott R, Ward DE, Babbitt R, Latham D (1991) Fire dynamics and chemistry of large fires. In 'Global Biomass Burning: Atmospheric, Climatic, and Biospheric Implications'. (Ed JS Levine) pp. 245–251. (The MIT Press: Cambridge, Mass)

Susott RA (1982) Differential scanning calorimetry of forest fuels. *Forest Science* **28**, 839–851.

Tachajapong W, Lozano J, Mahalingam S, Zhou X, Weise DR (2008) An investigation of crown fuel bulk density effects on the dynamics of crown fire initiation in shrublands. *Combustion Science and Technology* **180**, 593–615. doi:10.1080/00102200701838800

Tihay V, Gillard P (2011) Comparison of several kinetic approaches to evaluate the pyrolysis of three Mediterranean forest fuels. *International Journal of Wildland Fire* **20**, 407–417. doi:10.1071/WF09106

Tihay V, Santoni P-A, Simeoni A, Garo J-P, Vantelon J-P (2009) Skeletal and global mechanisms for the combustion of gases released by crushed forest fuels. *Combustion and Flame* **156**, 1565–1575. doi:10.1016/j.combustflame.2009.05.004

Tihay-Felicelli V, Santoni PA, Gerandi G, Barboni T (2017) Smoke emissions due to burning of green waste in the Mediterranean area: Influence of fuel moisture content and fuel mass. *Atmospheric Environment* **159**, 92–106. doi:10.1016/j.atmosenv.2017.04.002

Urbanski SP, Hao WM, Baker S (2008) Chemical composition of wildland fire emissions. In 'Wildland Fires and Air Pollution'. (Eds A Bytnerowicz, MJ Arbaugh, AR Riebau, C Andersen) Developments in Environmental Science. pp. 79–107. (Elsevier: Amsterdam, The Netherlands) doi:10.1016/S1474-8177(08)00004-1

van den Boogaart KG, Tolosana-Delgado R (2013) 'Analyzing compositional data with R.' (Springer: Heidelberg)

van Wilgen BW (1984) Adaptation of the United States Fire Danger Rating System to fynbos conditions: Part I. A fuel model for fire danger rating in the fynbos biome. *South African Forestry Journal* **129**, 61–65. doi:10.1080/00382167.1984.9628938

Wade D (1993) Thinning young loblolly pine stands with fire. *International Journal of Wildland Fire* **3**, 169. doi:10.1071/WF9930169

Wadhwani R, Sutherland D, Moinuddin KAM, Joseph P (2017) Kinetics of pyrolysis of litter materials from pine and eucalyptus forests. *Journal of Thermal Analysis and Calorimetry* **130**, 2035–2046. doi:10.1007/s10973-017-6512-0

Waldrop TA, Goodrick SL (2012) Introduction to prescribed fires in southern ecosystems. USDA Forest Service, Southern Research Station, Science Update SRS-054. (Asheville, NC). Available at http://www.treesearch.fs.fed.us/pubs/41316

Wang H, Lou S, Huang C, Qiao L, Tang X, Chen C, Zeng L, Wang Q, Zhou M, Lu S, Yu X (2014) Source profiles of volatile organic compounds from biomass burning in Yangtze River Delta, China. *Aerosol and Air Quality Research* **14**, 818–828. doi:10.4209/aaqr.2013.05.0174

Wang S, Dai G, Yang H, Luo Z (2017) Lignocellulosic biomass pyrolysis mechanism: A state-of-the-art review. *Progress in Energy and Combustion Science* **62**, 33–86. doi:10.1016/j.pecs.2017.05.004

Ward DE, Hao WM (1991) Projections of emissions from burning of biomass for use in studies of global climate and atmospheric chemistry. Paper 91-128.4. Presented at the 84th Annual Meeting and Exhibition; Vancouver, British Columbia; June 16–21, 1991. Air and Waste Management Association. Available at http://www.treesearch.fs.fed.us/pubs/43258

Ward DE, Radke LF (1993) Emissions measurement from vegetation fires: a comparative evaluation of methods and results. In 'Fire in the environment: the ecological, atmospheric, and climatic importance of vegetation fires: report of the Dahlem Workshop, held in Berlin, 15–20 March 1992'. (Eds PJ Crutzen, JG Goldammer) pp. 53–76. (John Wiley & Sons Ltd). Available at http://www.fs.fed.us/rm/pubs_other/rmrs_1993_ward_d001.pdf

Ward DE, Nelson Jr RM, Adams DF (1979) Forest fire smoke plume documentation. Paper No. 79-6.3. Proceedings 72nd Annual Meeting, 21–29 June 1979, Cincinnati, OH. (Air Pollution Control Association: Pittsburg, PA)

Ward DE, Susott RA, Kauffman JB, Babbitt RE, Cummings DL, Dias B, Holben BN, Kaufman YJ, Rasmussen RA, Setzer AW (1992) Smoke and fire characteristics for cerrado and deforestation burns in Brazil:

BASE-B Experiment. *Journal of Geophysical Research* **97**, 14601–14619. doi:10.1029/92JD01218.

Weise DR, Fletcher TH, Johnson TJ, Hao WM, Dietenberger M, Princevac M, Butler B, McAllister S, O'Brien J, Loudermilk L, Ottmar R, Hudak A, Kato A, Shotorban B, Mahalingam S, Mell WE (2018) A project to measure and model pyrolysis to improve prediction of prescribed fire behavior. In 'Advances in Forest Fire Research 2018' (Ed DX Viegas) pp. 308–318. (Coimbra University Press: Coimbra, Portugal) https://doi.org/10.14195/978-989-26-16-506_33

Weise DR, Jung H, Palarea-Albaladejo J, Cocker DR (2020*a*) Compositional data analysis of smoke emissions from debris piles with low-density polyethylene. *Journal of the Air & Waste Management Association* **0** (8), 834–845. doi:10.1080/10962247.2020.1784309

Weise DR, Palarea-Albaladejo J, Johnson TJ, Jung H (2020*b*) Analyzing wildland fire smoke emissions data using compositional data techniques. *Journal of Geophysical Research: Atmospheres* **125**, e2019JD032128. doi:10.1029/2019JD032128

Weise DR, Fletcher TH, Safdari M-S, Amini E, Palarea-Albaladejo J (2021) Application of compositional data analysis to determine the effects of heating mode, moisture status and plant species on pyrolysates. *International Journal of Wildland Fire* **31**(1), 24–45. doi:10.1071/WF20126

Westbrook CK, Dryer FL (1981) Simplified reaction mechanisms for the oxidation of hydrocarbon fuels in flames. *Combustion Science and Technology* **27**, 31–43. doi:10.1080/00102208108946970

Wooster M (2003) Fire radiative energy for quantitative study of biomass burning: derivation from the BIRD experimental satellite and comparison to MODIS fire products. *Remote Sensing of Environment* **86**, 83–107. doi:10.1016/S0034-4257(03)00070-1

Xiong S, Zhuo J, Zhang B, Yao Q (2013) Effect of moisture content on the characterization of products from the pyrolysis of sewage sludge. *Journal of Analytical and Applied Pyrolysis* **104**, 632–639. doi:10.1016/j.jaap.2013.05.003

Yashwanth BL, Shotorban B, Mahalingam S, Weise DR (2015) An investigation of the influence of heating modes on ignition and pyrolysis of woody wildland fuel. *Combustion Science and Technology* **187**, 780–796. doi:10.1080/00102202.2014.973948

Yashwanth BL, Shotorban B, Mahalingam S, Lautenberger CW, Weise DR (2016) A numerical investigation of the influence of radiation and moisture content on pyrolysis and ignition of a leaf-like fuel element. *Combustion and Flame* **163**, 301–316. doi:10.1016/j.combustflame.2015.10.006

Yokelson RJ, Goode JG, Ward DE, Susott RA, Babbitt RE, Wade DD, Bertschi I, Griffith DWT, Hao WM (1999) Emissions of formaldehyde, acetic acid, methanol, and other trace gases from biomass fires in North Carolina measured by airborne Fourier transform infrared spectroscopy. *Journal of Geophysical Research* **104**, 30109–30125. doi:10.1029/1999JD900817

Yokelson RJ, Burling IR, Gilman JB, Warneke C, Stockwell CE, de Gouw J, Akagi SK, Urbanski SP, Veres P, Roberts JM, Kuster WC, Reardon J, Griffith DWT, Johnson TJ, Hosseini S, Miller JW, Cocker DRIII, Jung H, Weise DR (2013) Coupling field and laboratory measurements to estimate the emission factors of identified and unidentified trace gases for prescribed fires. *Atmospheric Chemistry and Physics* **13**, 89–116. doi:10.5194/acp-13-89-2013

Zhou X, Mahalingam S (2001) Evaluation of reduced mechanism for modeling combustion of pyrolysis gas in wildland fire. *Combustion Science and Technology* **171**, 39–70. doi:10.1080/00102200108907858

Zhou X, Mahalingam S, Weise D (2005) Modeling of marginal burning state of fire spread in live chaparral shrub fuel bed. *Combustion and Flame* **143**, 183–198. doi:10.1016/j.combustflame.2005.05.013

Zhou XY, Pereira JCF (2000) A multidimensional model for simulating vegetation fire spread using a porous media sub-model. *Fire and Materials* **24**, 37–43. doi:10.1002/(SICI)1099-1018(200001/02)24:1<37::AID-FAM718>3.0.CO;2-Q

Zylstra P, Bradstock RA, Bedward M, Penman TD, Doherty MD, Weber RO, Gill AM, Cary GJ (2016) Biophysical mechanistic modelling quantifies the effects of plant traits on fire severity: species, not surface fuel loads, determine flame dimensions in eucalypt forests. *PLoS One* **11**, e0160715. (Ed G Bohrer)doi:10.1371/journal.pone.0160715

Appendix Fuels, fire behavior, gas composition and statistical tests associated with wind tunnel and field fires

Table A1. Properties and characteristics of wind tunnel and field fires burned to measure pyrolysis gases. Environmental conditions measured prior (less than 5 min) of start of experiment. Values rounded to appropriate number of significant digits.

Fire	Location	Fuel bed[A]	Wind[B]	Spread rate[C] ($m\ s^{-1}$)	Maximum temperature[D] (°C)	Heating rate[E] ($°C\ s^{-1}$)	Fuel moisture (%)		Air temperature (°C)	Relative humidity (%)
							Dead	Live		
3	RFL	Needles only	N	0.006			11		25.3	47
4	RFL	Needles only	N	0.006			12		22.6	52
5	RFL	Needles only	N	0.005			13		22.6	53
8	RFL	Needles only	N	0.004	439	95	15		20.4	67
9	RFL	Needles only	N	0.005	660	57	16		23.7	50
10	RFL	Needles only	N	0.006	578	85	11		22.6	50
11	RFL	Needles only	N	0.005	612	103	12		21.5	56
12	RFL	High Inkberry	N	0.005	615	282	11	117	20.4	56
13	RFL	Low Inkberry	N	0.005	398	51	12	120	18.7	62
14	RFL	High Inkberry	N	0.005	438	18	10	128	19.8	61
15	RFL	Low Inkberry	N	0.005	630	314	8	120	21.5	51
16	RFL	Low Inkberry	N	0.005	660	54	8	108	24.2	46
17	RFL	High Inkberry	N	0.006			8	116	24.2	35
18	RFL	High Inkberry	N	0.005	552	42	8	117	24.8	30
19	RFL	Low Inkberry	N	0.005	605	48	9	117	24.8	31
20	RFL	Low Inkberry	N	0.005	427	12	15	136	21.5	52
21	RFL	High Inkberry	N	0.005	660	66	14	104	22.0	42
22	RFL	Low Inkberry	N	0.006	563	33	12	99	24.2	34
23	RFL	High Inkberry	N	0.006	612	27	10	106	25.3	29
24	RFL	Low Inkberry	N	0.006	660	99	9	100	25.3	28
25	RFL	High Inkberry	N	0.006	616	72	10	122	25.3	33
26	RFL	Longleaf	Y	0.011	660	32	10		22.6	31
27	RFL	Longleaf	Y	0.010	590	107	10		21.5	31
28	RFL	Low Inkberry	Y	0.009	462	28	12	93	20.4	34
29	RFL	High Inkberry	Y	0.009	660	60	9	108	23.1	32
30	RFL	High Inkberry	Y	0.009	643	76	10	120	24.2	29
31	RFL	Low Inkberry	Y	0.009	590	59	7	133	26.4	21
32	RFL	High Inkberry	N	0.006	606	200	8	116	26.4	24
33	RFL	High Inkberry	Y	0.011	614	24	8	117	25.9	26
34	RFL	High Inkberry	Y	0.010	597	34	11	121	22.6	40
35	RFL	High Inkberry	N	0.005	557	23	10	113	23.1	42
36	RFL	High Inkberry	N	0.005	644	65	10	93	23.7	36
37	RFL	High Inkberry	N	0.005	660	42	10	124	26.4	29
38	RFL	High Inkberry	N	0.005	610	29	9	102	27.0	26

(*Continued on next page*)

Table A1. (*Continued*)

Fire	Location	Fuel bed[A]	Wind[B]	Spread rate[C] ($m\ s^{-1}$)	Maximum temperature[D] (°C)	Heating rate[E] ($°C\ s^{-1}$)	Fuel moisture (%)		Air temperature (°C)	Relative humidity (%)
							Dead	Live		
41	RFL	Blueberry	N	0.005	508	15	10	118	26.4	33
42	RFL	Blueberry	N	0.006	524	148	10	130	27.0	33
44	RFL	Fetterbush	N	0.005	645	38	9	104	25.9	42
45	RFL	Fetterbush	N	0.006	545	29	6	106	24.2	42
46	RFL	Fetterbush Blueberry	N	0.004	569	20	12	135	18.7	37
47	RFL	Fetterbush	N	0.005	482	18	11	105	21.5	31
48	RFL	Fetterbush Blueberry	N	0.006	602	25	10	131	23.1	25
49	RFL	Fetterbush	N	0.006	638	48	10	103	24.2	49
51	RFL	Longleaf	Y	0.015	430	55	11		6.7	75
52	RFL	Fetterbush	Y	0.015	567	65	10	79	6.1	59
53	RFL	Blueberry	Y	0.018	414	208	11	148	11.7	39
55	RFL	Fetterbush	Y	0.019	509		10		6.1	43
56	RFL	Longleaf	Y	0.018	660	167	10		9.4	35
57	RFL	Blueberry	Y	0.017	528	48	12	130	5.6	73
58	RFL	Fetterbush Blueberry	Y	0.027	417	39	11	138	5.6	70
59	RFL	Longleaf	Y	0.017	532	291	11		7.8	58
60	RFL	Fetterbush	Y	0.020	660	88	10	103	8.3	50
61	RFL	Fetterbush Blueberry	Y	0.021	472	140	10	127	6.7	67
62	RFL	Longleaf	Y	0.019	513	378	10		6.7	63
63	RFL	Blueberry	Y	0.016	218	171	12	128	7.2	63
64	RFL	Fetterbush	Y	0.015	315	329	12	93	6.1	73
65	RFL	Fetterbush Blueberry	Y	0.017	523	148	10	139	6.7	62
66	RFL	Blueberry	Y	0.019	479	113	11	137	7.2	63
67	RFL	Longleaf	Y	0.020	514	72	10		7.2	63
68	RFL	Fetterbush	Y	0.022	601	102	10	103	7.8	63
69	RFL	Fetterbush	Y	0.016	471	443	12	102	7.8	78
70	RFL	Blueberry	Y	0.017	478	179	11	150	7.8	78
71	RFL	Fetterbush Blueberry	Y	0.016	341	39	12	132	6.1	73
72	RFL	Blueberry	Y	0.018	533	43	9	128	8.3	74
73	RFL	Fetterbush Blueberry	Y	0.023	516	17	9	107	10.0	65
74	RFL	Longleaf	Y	0.011	419	400	12		20.0	96
75	RFL	Longleaf	Y	0.009	405	104	13		20.8	59
76	RFL	High Inkberry	Y	0.010	373	10	12	97	23.9	48

(*Continued on next page*)

Table A1. (*Continued*)

Fire	Location	Fuel bed[A]	Wind[B]	Spread rate[C] ($m\ s^{-1}$)	Maximum temperature[D] (°C)	Heating rate[E] ($°C\ s^{-1}$)	Fuel moisture (%)		Air temperature (°C)	Relative humidity (%)
							Dead	Live		
77	RFL	Fetterbush	Y	0.009	648	21	9	106	28.3	35
78	RFL	Sparkleberry	Y	0.010	304	16	9	105	28.9	19
79	RFL	High Inkberry	Y	0.010	190	39	9	100	28.3	26
80	RFL	Sparkleberry	Y	0.011	435	8	9	108	23.2	15
81	RFL	Fetterbush	Y	0.011	273	75	7	79	23.3	12
82	RFL	Sparkleberry	Y	0.009	132	49	8	107	25.6	12
83	RFL	High Inkberry	Y	0.010	343	23	7	92	27.8	11
84	RFL	Fetterbush	Y	0.010		41	8	135	27.8	10
85	RFL	Fetterbush	Y	0.010	294	22	7	102	28.9	9
86	RFL	Sparkleberry	Y	0.013	288	21	7	100	13.9	33
87	RFL	High Inkberry	Y	0.014	419	56	8	92	12.8	33
88	RFL	Fetterbush	Y	0.014	199	52	7	99	12.8	39
89	RFL	High Inkberry	Y	0.011	630	37	7	89	29.4	18
90	RFL	Sparkleberry	Y	0.008	468	20	7	106	28.9	19
91	RFL	Fetterbush	Y	0.009	236	48	8	109	29.4	18
92	RFL	High Inkberry	Y	0.010	612	58	9	95	21.7	30
93	RFL	Fetterbush	Y	0.009	223	4	8	89	26.1	24
94	RFL	Sparkleberry	Y	0.009	648	94	8	111	29.4	23
95	RFL	Sparkleberry	Y	0.012	526	28	7	116	25.6	24
96	RFL	Fetterbush	Y	0.012	388	5	8	88	28.9	21
97	RFL	Sparkleberry	Y	0.011	439	11	8	86	28.9	22
101	TTRS	Subxeric Woodland	Y						28	25
102	TTRS	Subxeric Woodland	Y						28	25
201	FJSC	Fall-line Sandhills	Y				7	211	24	26
202	FJSC	Fall-line Sandhills	Y		599	259	7	211	28	18
203	FJSC	Fall-line Sandhills	Y				12	212	21	53
204	FJSC	Fall-line Sandhills	Y		648	372	12	212	27	34
205	FJSC	Fall-line Sandhills	Y		264	107	13	177	22	59
206	FJSC	Fall-line Sandhills	Y		231	117	6	191	26	43
207	FJSC	Fall-line Sandhills	Y		264	107	6	191	29	30

[A]Each wind tunnel fuel bed contained 1000 g of longleaf pine needles. After adjusting for fuel moisture content, longleaf pine needle mass ranged from 862 to 943 g. Fuel consumption was not measured; however, virtually all longleaf pine needle mass was consumed by flaming combustion with minimal residual smouldering combustion. Fort Jackson (FJSC) and Tall Timbers Pebble Hill Plantation (TTRS) classification from Peet and Allard (1993); Ostertag and Robertson (2007).

[B]N = no concurrent air flow, Y = concurrent air flow of nominally 1 $m\ s^{-1}$.

[C]Calculated quasi-steady fire rate of spread (fuel bed length/transit time).

[D]Maximum uncorrected radiometric leaf temperature (T_i) measured by 7–13 μm thermal camera.

[E]Maximum heating rate = $\max[(T_i - T_{i-1})/(t_i - t_{i-1})]$, $T_i > T_{i-1}$.

Table A2. Size measurements of plants used in wind tunnel pyrolysis experiment. Sample size of 40 plants per species. Values are arithmetic mean (standard deviation).

Species	Crown[A]			
	Height (cm)	Diameter 1 (cm)	Diameter 2 (cm)	Area (cm^2)
Ilex glabra	17.0 (2.6)	11.2	9.7	318.4
Lyonia lucida	22.7 (2.9)	18.5	16.4	856.7
Vaccinium arboreum	20.6 (2.6)	18.9	15.8	879.8

[A]The planform projection of a plant crown was assumed to be an ellipse. Two diameters (diameter 1 = maximum crown diameter and crown diameter 2 measured perpendicular to crown diameter 1) estimated crown area = $\pi d_1 d_2$.

Table A3. Pre and postburn fuel loading by component (g m^{-2}) for four 0.1 ha burn units in longleaf pine forest at Fort Jackson, SC.

Component	Fuel loading					Centre[B]	Var[C]
	Burn unit				Mean ⁎ s.d.[A]		
	24A	24B	16D1	16D5			
Preburn							
Litter	885.1	499.8	575.8	405.6	566.9⁎1.4	3.39×10^{-1}	2.0
Duff	5155.1	616.0	1909.2	161.6	994.9⁎4.4	5.94×10^{-1}	7.7
Cones	0.1	0.1	12.7	17.0	1.2⁎18.2	7.15×10^{-4}	20.3
Suspended litter	0.2	6.4	0.1	0.2	0.4⁎6.4	2.36×10^{-4}	13.5
1 h	1.6	5.0	24.7	18.2	7.7⁎3.5	4.63×10^{-3}	5.8
10 h	64.9	42.2	127.6	119.1	80.3⁎1.7	4.80×10^{-2}	1.9
100 h	0.0	0.8	0.0	0.1	0.0⁎19.5	1.53×10^{-5}	19.2
1000 h	0.0	0.0	0.0	0.0	0.0⁎2.5	9.51×10^{-7}	6.0
Herbs	0.0	73.4	0.0	0.0	0.0⁎209.4	1.66×10^{-5}	18.4
Shrubs	22.3	60.4	1.7	125.7	23.3⁎6.5	1.39×10^{-2}	5.2
Postburn							
Litter	58.5	20.6	3.3	17.1	16.2⁎3.3	1.82×10^{-2}	6.6
Duff	4843.4	436.6	1762.7	141.4	852.0⁎4.7	9.57×10^{-1}	6.8
Cones	0.0	0.0	0.2	0.1	0.0⁎4.7	4.42×10^{-5}	16.1
Suspended litter	0.0	0.0	0.0	0.0	0.0⁎2.5	2.31×10^{-6}	4.5
1 h	0.0	0.0	0.1	0.0	0.0⁎7.6	1.03×10^{-5}	9.6
10 h	44.6	22.6	4.7	30.9	19.6⁎2.7	2.20×10^{-2}	2.8
100 h	0.1	2.1	0.1	0.4	0.3⁎4.7	3.15×10^{-4}	30.0
1000 h	0.0	0.0	0.0	0.0	0.0⁎1.0	1.12×10^{-6}	1.2
Herbs	0.0	0.1	0.0	0.0	0.0⁎8.8	4.50×10^{-6}	7.9
Shrubs	1.2	14.6	0.4	5.9	2.5⁎5.1	2.81×10^{-3}	14.5

[A]Geometric mean is related to geometric standard deviation by multiplication and division, represented by '⁎'.
[B]Centre (mean) composition for four 0.1 ha plots. Eight sample points located in each burn unit. Each value (dimensionless) indicates the relative proportion of the fuel component. Formulae for the centre and metric variance can be found elsewhere (Aitchison 1986).
[C]Percentage of metric variance (mvar) contributed by fuel component (unitless).

Table A4. Summary statistics for pyrolysis and flaming combustion canisters collected during fires in longleaf pine fuel beds. Concentration in parts per million (ppm).

Gas	Concentration[A]			BDL[B]	Wind tunnel			
					Centre[C]		Var[D]	
	Wind tunnel	Fort Jackson	Pebble Hill		Pyro	Flam	Pyro	Flam
Carbon dioxide (CO_2)	$3.84 \times 10^{3} \divideontimes 4.82 \times 10^{0}$	$1.18 \times 10^{3} \divideontimes 2.34 \times 10^{0}$	$4.06 \times 10^{3} \divideontimes 3.17 \times 10^{0}$	0.0	9.28×10^{-1}	9.47×10^{-1}	3.6	2.8
Carbon monoxide (CO)	$1.80 \times 10^{2} \divideontimes 1.34 \times 10^{1}$	$1.82 \times 10^{1} \divideontimes 7.31 \times 10^{0}$	$2.62 \times 10^{2} \divideontimes 1.25 \times 10^{1}$	0.0	4.82×10^{-2}	3.91×10^{-2}	3.0	3.5
Hydrogen (H_2)	$4.32 \times 10^{1} \divideontimes 1.07 \times 10^{1}$	$3.27 \times 10^{0} \divideontimes 3.98 \times 10^{0}$	$4.75 \times 10^{1} \divideontimes 1.21 \times 10^{1}$	0.0	1.47×10^{-2}	6.87×10^{-3}	1.6	1.9
Methane (CH_4)	$2.20 \times 10^{1} \divideontimes 6.86 \times 10^{0}$	$3.69 \times 10^{0} \divideontimes 1.87 \times 10^{0}$	$2.69 \times 10^{1} \divideontimes 7.44 \times 10^{0}$	0.0	6.07×10^{-3}	4.60×10^{-3}	0.8	0.8
Ethane (C_2H_6)	$9.14 \times 10^{-1} \divideontimes 1.27 \times 10^{1}$	$9.24 \times 10^{-2} \divideontimes 4.19 \times 10^{0}$	$1.41 \times 10^{0} \divideontimes 1.13 \times 10^{1}$	8.1	2.81×10^{-4}	1.72×10^{-4}	0.2	0.4
Ethylene (C_2H_4)	$6.33 \times 10^{0} \divideontimes 1.81 \times 10^{1}$	$3.91 \times 10^{-1} \divideontimes 9.69 \times 10^{0}$	$1.05 \times 10^{1} \divideontimes 1.61 \times 10^{1}$	3.5	1.88×10^{-3}	1.14×10^{-3}	0.8	2.0
Acetylene (C_2H_2)	$1.74 \times 10^{0} \divideontimes 1.45 \times 10^{1}$	$1.84 \times 10^{-1} \divideontimes 6.57 \times 10^{0}$	$3.22 \times 10^{0} \divideontimes 3.80 \times 10^{1}$	7.6	4.80×10^{-4}	4.12×10^{-4}	3.5	3.6
Propane (C_3H_8)	$2.56 \times 10^{-1} \divideontimes 1.83 \times 10^{1}$	$1.74 \times 10^{-2} \divideontimes 5.21 \times 10^{1}$	$1.81 \times 10^{-1} \divideontimes 8.84 \times 10^{0}$	11.6	8.33×10^{-5}	4.29×10^{-5}	2.0	1.8
Propylene (C_3H_6)	$2.93 \times 10^{-1} \divideontimes 1.47 \times 10^{1}$	$8.14 \times 10^{-2} \divideontimes 8.34 \times 10^{0}$	$9.82 \times 10^{-1} \divideontimes 3.82 \times 10^{1}$	17.7	8.56×10^{-5}	5.25×10^{-5}	7.3	6.8
Propyne (C_3H_4)	$1.88 \times 10^{-1} \divideontimes 1.82 \times 10^{1}$	$1.57 \times 10^{-2} \divideontimes 5.94 \times 10^{0}$	$1.70 \times 10^{-1} \divideontimes 1.84 \times 10^{1}$	19.7	6.01×10^{-5}	3.38×10^{-5}	0.7	1.9
Butane (C_4H_{10})	$6.72 \times 10^{-2} \divideontimes 1.59 \times 10^{1}$	$7.97 \times 10^{-3} \divideontimes 5.26 \times 10^{0}$	$1.37 \times 10^{-1} \divideontimes 1.27 \times 10^{1}$	27.8	2.24×10^{-5}	1.22×10^{-5}	1.1	2.5
Isobutane (C_4H_{10})	$2.07 \times 10^{-2} \divideontimes 1.34 \times 10^{2}$	$6.68 \times 10^{-4} \divideontimes 3.40 \times 10^{1}$	$4.27 \times 10^{-3} \divideontimes 1.78 \times 10^{1}$	50.0	3.50×10^{-6}	3.73×10^{-6}	25.2	15.0
Butene (C_4H_8)	$1.41 \times 10^{-1} \divideontimes 1.21 \times 10^{1}$	$2.17 \times 10^{-2} \divideontimes 4.68 \times 10^{0}$	$2.04 \times 10^{-1} \divideontimes 1.72 \times 10^{1}$	14.1	4.42×10^{-5}	2.35×10^{-5}	0.5	0.9
Isobutene (C_4H_8)	$7.30 \times 10^{-2} \divideontimes 9.03 \times 10^{0}$	$2.07 \times 10^{-2} \divideontimes 2.75 \times 10^{0}$	$1.26 \times 10^{-1} \divideontimes 1.05 \times 10^{1}$	17.7	2.12×10^{-5}	1.23×10^{-5}	1.7	1.3
*trans*2butene (C_4H_8)	$4.84 \times 10^{-2} \divideontimes 2.04 \times 10^{1}$	$2.27 \times 10^{-3} \divideontimes 1.12 \times 10^{1}$	$4.77 \times 10^{-2} \divideontimes 1.08 \times 10^{1}$	31.3	1.40×10^{-5}	8.41×10^{-6}	2.8	1.7
*cis*2butene (C_4H_8)	$1.82 \times 10^{-2} \divideontimes 9.46 \times 10^{0}$	$7.30 \times 10^{-3} \divideontimes 2.89 \times 10^{0}$	$3.36 \times 10^{-2} \divideontimes 1.41 \times 10^{1}$	37.9	5.03×10^{-6}	4.93×10^{-6}	3.7	1.9
Butadiene (C_4H_6)	$1.05 \times 10^{-1} \divideontimes 1.22 \times 10^{1}$	$2.70 \times 10^{-2} \divideontimes 4.25 \times 10^{0}$	$2.97 \times 10^{-1} \divideontimes 1.95 \times 10^{1}$	18.2	3.38×10^{-5}	1.60×10^{-5}	3.6	3.5
Pentane (C_5H_{12})	$1.28 \times 10^{-2} \divideontimes 5.78 \times 10^{1}$	$1.26 \times 10^{-4} \divideontimes 2.71 \times 10^{1}$	$6.17 \times 10^{-3} \divideontimes 7.98 \times 10^{1}$	52.5	3.69×10^{-6}	1.67×10^{-6}	9.3	8.0
Isopentane (C_5H_{12})	$2.13 \times 10^{-3} \divideontimes 2.95 \times 10^{2}$	$3.84 \times 10^{-4} \divideontimes 6.14 \times 10^{1}$	$1.15 \times 10^{-3} \divideontimes 2.91 \times 10^{1}$	58.1	1.21×10^{-6}	1.84×10^{-7}	18.8	26.9
Pentene (C_5H_{10})	$2.17 \times 10^{-2} \divideontimes 1.37 \times 10^{1}$	$3.81 \times 10^{-3} \divideontimes 7.88 \times 10^{0}$	$4.27 \times 10^{-2} \divideontimes 1.28 \times 10^{1}$	40.9	6.43×10^{-6}	3.81×10^{-6}	2.5	1.7
*trans*2pentene (C_5H_{10})	$7.56 \times 10^{-3} \divideontimes 2.42 \times 10^{1}$	$2.31 \times 10^{-3} \divideontimes 6.83 \times 10^{0}$	$3.35 \times 10^{-2} \divideontimes 6.34 \times 10^{0}$	58.6	2.31×10^{-6}	1.26×10^{-6}	3.3	7.1
*cis*2pentene (C_5H_{10})	$6.56 \times 10^{-3} \divideontimes 1.83 \times 10^{1}$	$7.43 \times 10^{-4} \divideontimes 1.19 \times 10^{1}$	$6.63 \times 10^{-3} \divideontimes 2.72 \times 10^{1}$	61.1	2.01×10^{-6}	8.00×10^{-7}	3.9	4.1

[A]Geometric mean is related to geometric standard deviation by multiplication and division, represented by '$\divideontimes$'.
[B]Percentage of observations with below detection limit (BDL) values.
[C]Mean (centre) composition for pyrolysis and flaming combustion canisters based on concentration. Values are unitless proportions.
[D]Percentage of metric variance contributed by pyrolysate.

Table A5. Variation array of gas composition for pyrolysis and flaming combustion measured in a wind tunnel. Mean log-ratio and log-ratio variance ($\hat{\tau}_{ij}$) for each pair of gases are found below and above the diagonal, respectively.

	CO_2	CO	H_2	CH_4	C_2H_6	C_2H_4	C_2H_2	C_3H_8	C_3H_6	Propyne	Butane	Isobutane	*1*-butene	Isobutene	*trans*2-butene	*cis*2-butene	C_4H_6	Pentane	Isopentane	C_5H_{10}	*trans*2-pentene	*cis*2-pentene
Pyrolysis																						
CO_2		1.4[B]	2.4	1.6	3.1	4.4	4.3	4.6	6.5	3.9	3.3	22.7	3.0	2.3	7.2	2.6	4.2	11.7	24.0	4.3	6.1	5.4
CO	−3.0[A]		2.0	2.5	2.8	3.2	4.9	4.2	7.7	3.1	3.2	19.2	2.7	2.9	5.3	3.4	5.2	9.9	20.0	4.1	5.9	4.5
H_2	−4.1	−1.2		1.1	1.3	1.7	3.0	3.0	6.5	1.3	1.4	18.1	1.3	1.5	3.9	2.9	3.4	8.3	20.4	3.2	4.3	3.6
CH_4	−5.0	−2.1	−0.9		0.6	1.5	2.5	2.1	5.6	1.2	1.1	18.5	0.8	0.9	4.3	2.1	2.8	7.5	20.5	2.0	3.0	2.9
C_2H_6	−8.1	−5.2	−4.0	−3.1		0.4	2.3	1.3	5.7	0.6	0.8	16.3	0.2	1.2	2.7	2.8	3.3	5.9	18.5	1.7	2.6	2.2
C_2H_4	−6.2	−3.2	−2.1	−1.2	1.9		2.7	1.9	6.6	0.5	1.2	16.4	0.8	2.1	2.3	3.6	4.1	5.5	18.0	2.5	3.3	2.8
C_2H_2	−7.6	−4.6	−3.4	−2.5	0.6	−1.4		6.2	1.6	2.0	1.4	27.8	1.9	1.4	6.9	2.4	1.9	12.0	29.3	4.3	5.1	4.9
C_3H_8	−9.3	−6.3	−5.2	−4.3	−1.2	−3.1	−1.7		10.6	2.5	3.0	12.3	1.8	3.4	2.3	5.7	6.9	5.3	15.2	3.1	4.0	3.3
C_3H_6	−9.4	−6.4	−5.2	−4.3	−1.3	−3.2	−1.8	−0.1		5.6	4.6	35.4	5.0	3.9	11.8	3.9	3.6	17.9	36.3	7.3	8.6	8.6
Propyne	−9.7	−6.7	−5.5	−4.7	−1.6	−3.5	−2.1	−0.4	−0.3		0.7	17.5	0.7	1.6	2.9	3.3	3.2	6.4	20.2	2.3	3.2	2.7
Butane	−10.6	−7.7	−6.5	−5.6	−2.5	−4.4	−3.1	−1.3	−1.3	−0.9		19.9	0.6	1.0	3.8	2.4	2.6	7.9	21.8	2.5	3.3	2.8
Isobutane	−12.2	−9.2	−8.0	−7.2	−4.1	−6.0	−4.6	−2.9	−2.8	−2.5	−1.6		17.2	21.5	13.2	24.5	27.2	14.2	14.6	16.7	16.8	17.3
Butene	−9.9	−7.0	−5.8	−4.9	−1.8	−3.7	−2.4	−0.6	−0.6	−0.3	0.7	2.3		0.9	2.7	2.4	2.9	6.5	19.1	1.4	2.5	2.4
Isobutene	−10.6	−7.6	−6.5	−5.6	−2.5	−4.4	−3.0	−1.3	−1.2	−0.9	0.0	1.6	−0.7		4.9	1.4	1.0	9.4	23.1	2.4	3.6	3.4
*trans*2butene	−11.3	−8.3	−7.1	−6.2	−3.1	−5.1	−3.7	−2.0	−1.9	−1.6	−0.6	0.9	−1.3	−0.7		6.7	7.8	4.6	14.5	4.0	5.0	4.8
*cis*2butene	−12.0	−9.1	−7.9	−7.0	−3.9	−5.8	−4.5	−2.7	−2.6	−2.3	−1.4	0.2	−2.1	−1.4	−0.8		2.4	11.5	24.4	3.9	5.2	5.4
C_4H_6	−10.1	−7.2	−6.0	−5.1	−2.0	−3.9	−2.6	−0.8	−0.7	−0.4	0.5	2.1	−0.2	0.5	1.1	1.9		13.1	28.8	4.7	6.1	6.1
Pentane	−12.2	−9.2	−8.0	−7.2	−4.1	−6.0	−4.6	−2.9	−2.8	−2.5	−1.6	0.0	−2.2	−1.6	−0.9	−0.2	−2.1		17.2	6.9	8.8	7.2
Isopentane	−13.7	−10.7	−9.5	−8.7	−5.6	−7.5	−6.1	−4.4	−4.3	−4.0	−3.1	−1.5	−3.7	−3.1	−2.4	−1.7	−3.6	−1.5		18.2	21.0	19.6
C_5H_{10}	−11.9	−8.9	−7.7	−6.8	−3.7	−5.7	−4.3	−2.6	−2.5	−2.2	−1.2	0.3	−1.9	−1.3	−0.6	0.2	−1.7	0.3	1.8		3.6	3.0
*trans*2-pentene	−12.7	−9.7	−8.6	−7.7	−4.6	−6.5	−5.1	−3.4	−3.3	−3.0	−2.1	−0.5	−2.8	−2.1	−1.5	−0.7	−2.6	−0.5	1.0	−0.8		3.5
*cis*2pentene	−13.1	−10.1	−8.9	−8.0	−4.9	−6.9	−5.5	−3.8	−3.7	−3.4	−2.4	−0.9	−3.1	−2.5	−1.8	−1.0	−2.9	−0.9	0.6	−1.2	−0.4	
Flaming combustion																						
CO_2		1.7	2.1	1.4	3.7	5.0	3.7	6.2	4.6	5.4	4.3	24.4	3.6	3.2	6.6	3.9	4.5	18.6	31.8	3.6	8.2	4.9
CO	−3.2		2.8	2.5	4.1	4.8	3.9	7.3	4.9	5.5	4.4	25.7	4.5	3.9	7.2	5.2	4.6	19.9	34.1	4.6	9.2	6.4
H_2	−4.9	−1.7		1.4	1.9	3.2	2.8	4.9	3.9	2.8	2.7	22.4	2.1	2.0	4.9	4.1	3.4	17.3	33.7	3.0	9.2	5.1
CH_4	−5.3	−2.1	−0.4		1.3	2.6	3.3	3.5	5.4	2.8	2.2	18.4	1.3	1.6	3.6	2.6	2.4	14.5	29.2	1.8	6.4	3.4
C_2H_6	−8.7	−5.5	−3.7	−3.3		1.1	2.7	1.9	5.7	1.0	2.1	17.2	0.7	1.1	2.7	2.8	2.3	13.4	29.9	1.9	7.0	4.6

(*Continued on next page*)

Table A5. (*Continued*)

	CO_2	CO	H_2	CH_4	C_2H_6	C_2H_4	C_2H_2	C_3H_8	C_3H_6	Propyne	Butane	Isobutane	*1*-butene	Isobutene	*trans*2-butene	*cis*2-butene	C_4H_6	Pentane	Isopentane	C_5H_{10}	*trans*2-pentene	*cis*2-pentene
C_2H_4	−6.7	−3.5	−1.8	−1.4	1.9		3.1	2.3	6.2	1.4	3.0	17.5	2.2	2.3	4.2	4.1	3.1	14.8	33.1	3.6	8.3	6.6
C_2H_2	−7.8	−4.6	−2.8	−2.4	0.9	−1.0		7.3	1.9	2.8	2.7	27.7	3.6	2.3	8.0	4.4	3.2	22.4	42.1	5.4	12.1	8.6
C_3H_8	−10.0	−6.8	−5.1	−4.7	−1.4	−3.3	−2.3		10.5	3.0	5.6	14.2	2.5	3.4	3.2	5.3	5.2	12.2	27.5	3.5	6.8	6.0
C_3H_6	−9.7	−6.6	−4.8	−4.4	−1.1	−3.0	−2.0	0.3		5.2	4.9	35.2	5.5	3.9	10.7	6.1	4.7	26.4	48.8	7.2	14.4	9.9
Propyne	−10.2	−7.1	−5.3	−4.9	−−1.6	−3.5	−2.5	−0.2	−0.5		2.3	19.6	1.3	1.6	3.5	3.9	2.7	16.4	35.4	3.5	9.2	6.7
Butane	−11.2	−8.0	−6.3	−5.9	−2.5	−4.5	−3.4	−1.2	−1.5	−1.0		22.6	1.9	2.0	5.4	3.9	2.7	18.9	36.7	3.4	8.8	5.8
Isobutane	−12.8	−9.6	−7.9	−7.5	−4.1	−6.1	−5.0	−2.7	−3.0	−2.5	−1.6		18.6	21.9	15.1	20.9	25.3	15.1	29.9	18.3	20.1	19.8
Butene	−10.5	−7.4	−5.6	−5.2	−1.9	−3.8	−2.8	−0.5	−0.8	−0.3	0.7	2.2		0.7	2.9	2.7	2.3	13.9	31.0	1.6	6.6	3.6
Isobutene	−11.3	−8.1	−6.4	−6.0	−2.6	−4.6	−3.5	−1.3	−1.5	−1.0	−0.1	1.5	−0.7		4.0	2.4	2.0	16.3	33.6	2.3	7.3	4.9
*trans*2butene	−11.8	−8.6	−6.8	−6.4	−3.1	−5.0	−4.0	−1.7	−2.0	−1.5	−0.6	1.0	−1.2	−0.5		4.8	5.8	10.6	25.8	3.5	6.8	6.2
*cis*2butene	−12.4	−9.2	−7.5	−7.1	−3.7	−5.7	−4.6	−2.4	−2.7	−2.2	−1.2	0.4	−1.9	−1.1	−0.6		3.0	15.0	32.1	3.2	7.4	5.7
C_4H_6	−10.9	−7.7	−6.0	−5.6	−2.2	−4.2	−3.1	−0.9	−1.1	−0.6	0.3	1.9	−0.3	0.4	0.9	1.5		18.6	38.7	3.8	9.1	6.7
Pentane	−13.8	−10.7	−8.9	−8.5	−5.2	−7.1	−6.1	−3.8	−4.1	−3.6	−2.6	−1.1	−3.3	−2.6	−2.1	−1.4	−3.0		23.3	13.0	10.4	11.0
Isopentane	−14.8	−11.7	−9.9	−9.5	−6.2	−8.1	−7.1	−4.8	−5.1	−4.6	−3.6	−2.1	−4.3	−3.6	−3.1	−2.4	−4.0	−1.0		27.0	23.0	28.5
C_5H_{10}	−12.4	−9.3	−7.5	−7.1	−3.8	−5.7	−4.7	−2.4	−2.7	−2.2	−1.2	0.3	−1.9	−1.2	−0.7	0.0	−1.6	1.4	2.4		6.2	4.3
*trans*2-pentene	−13.8	−10.6	−8.9	−8.5	−5.1	−7.1	−6.0	−3.8	−4.1	−3.6	−2.6	−1.0	−3.3	−2.5	−2.0	−1.4	−2.9	0.0	1.0	−1.4		5.3
*cis*2pentene	−13.6	−10.4	−8.7	−8.3	−4.9	−6.9	−5.8	−3.6	−3.8	−3.3	−2.4	−0.8	−3.0	−2.3	−1.8	−1.2	−2.7	0.3	1.3	−1.1	0.2	

[A]Geometric mean of log ratio.

[B]$\hat{\tau}_{ij}$ = var(ln(x_i/x_j)) where x_i and x_j are gases in the composition and var is the usual sample variance. exp($-\hat{\tau}_{ij}^2/2$) has been suggested as a measure of proportionality between two gases (van den Boogaart and Tolosana-Delgado 2013).

Table A6. Influence of fuel bed type and environmental variables on the composition of pyrolysis gases measured in a wind tunnel.

Source	d.f.[A]	Pillai's[B] trace	Hypothesis tests			
			F[C]	Num. d.f.	Den. d.f.	$P_r(>F)$
Fuel bed	6	1.90	1.35	126	366	0.02
Air temperature	1	0.31	2.65	21	56	0.27
Dead fuel moisture	1	0.36	1.74	21	56	0.12
Relative humidity	1	0.22	0.53	21	56	0.77

[A]Degrees of freedom of effect. Natural logarithms of air temperature, dead fuel moisture and relative humidity were used because they are ratio scale variables (van den Boogaart and Tolosana-Delgado 2013). Live fuel moisture and fuel temperature were initially included and were not significant covariates for individual gas log-ratios. Covariates not presented here due to numerical failure to estimate these effects in the global MANOVA presented here.
[B]Pillai's trace used to test equality of means.
[C]F-statistic associated with Pillai's trace. Numerator d.f. is the d.f. for the effect multiplied by $D - 1$.

Table A7. Effects of fire phase and location on composition of gases measured in a wind tunnel and in the field. These results apply to all *ilr* transformations including the balances in Table 1.

Source	d.f.[A]	Pillai's[B] trace	Hypothesis tests			
			F[C]	Num. d.f.	Den. d.f.	Pr(>F)
Location	2	0.53	2.98	42	344	<0.0001
Fire phase	1	0.33	4.08	21	171	<0.0001

[A]Degrees of freedom of effect.
[B]Pillai's trace used to test equality of means.
[C]F-statistic associated with Pillai's trace. Numerator d.f. is the d.f. for the effect multiplied by $D - 1$.

Data availability. Once approved for release by the sponsor of this study (SERDP), the data will be available through the Forest Service Research Data Archive, https://www.fs.usda.gov/rds/archive/.

Conflicts of interest. Andrew T. Hudak is an Associate Editor of International Journal of Wildland Fire but was blinded from the peer-review process for this paper. The authors declare no other conflicts of interest.

Declaration of funding. This work was supported by the DOD/DOE/EPA Strategic Environmental Research and Development Program project RC-2640. JPA was partly supported by the Scottish Government's Rural and Environment Science and Analytical Services Division and the Spanish Ministry of Science, Innovation and Universities under the project CODAMET (RTI2018-095518-B-C21, 2019-2021). USDA Forest Service annual research appropriations provided in-kind support from 2016 to 2021.

Author affiliations
[A]USDA Forest Service, Pacific Southwest Research Station, Riverside, CA 92507, USA
[B]USDA Forest Service, Rocky Mountain Research Station, Missoula, MT, USA.
[C]Department of Mechanical Engineering, University of California, Riverside, CA, USA.
[D]Biomathematics and Statistics Scotland, Edinburgh, Scotland, UK.
[E]Department of Computer Science, Applied Mathematics and Statistics, University of Girona, Girona, Catalonia, Spain.
[F]USDA Forest Service, Pacific Northwest Research Station, Seattle, WA, USA.
[G]USDA Forest Service, Rocky Mountain Research Station, Moscow, ID, USA.
[H]California Department of Forestry and Fire Protection, Fire and Resource Assessment Program, South Lake Tahoe, CA 96150, USA.
[I]USDA Forest Service, Southern Research Station, Athens, GA, USA.